Device Performance of Emerging Photovoltaic Materials (Version 3)

Osbel Almora,* Derya Baran, Guillermo C. Bazan, Carlos I. Cabrera, Sule Erten-Ela, Karen Forberich, Fei Guo, Jens Hauch, Anita W. Y. Ho-Baillie, T. Jesper Jacobsson, Rene A. J. Janssen, Thomas Kirchartz, Nikos Kopidakis, Maria A. Loi, Richard R. Lunt, Xavier Mathew, Michael D. McGehee, Jie Min, David B. Mitzi, Mohammad K. Nazeeruddin, Jenny Nelson, Ana F. Nogueira, Ulrich W. Paetzold, Barry P. Rand, Uwe Rau, Henry J. Snaith, Eva Unger, Lídice Vaillant-Roca, Chenchen Yang, Hin-Lap Yip, and Christoph J. Brabec*

Following the 2nd release of the "Emerging PV reports," the best achievements in the performance of emerging photovoltaic devices in diverse emerging photovoltaic research subjects are summarized, as reported in peer-reviewed articles in academic journals since August 2021. Updated graphs, tables, and analyses are provided with several performance parameters, e.g., power conversion efficiency, open-circuit voltage, short-circuit current density, fill factor, light utilization efficiency, and stability test energy yield. These parameters are presented as a function of the photovoltaic bandgap energy and the average visible transmittance for each technology and application, and are put into perspective using, e.g., the detailed balance efficiency limit. The 3rd installment of the "Emerging PV reports" extends the scope toward triple junction solar cells.

1. Introduction

Emerging photovoltaic (e-PV) technologies are arguably the main focus of the research community in the PV field as they hold the promise for providing cheap and scalable technologies for the photovoltaic commodity market as well as new and versatile applications such as flexible, transparent, and integrated photovoltaics. The state-of-the-art achievements as published in academic journals with data about the best performing devices in the research of e-PV devices have now been systematically parameterized and reported

O. Almora
Department of Physical, Chemical and Natural Systems
University Pablo de Olavide
Seville 41013, Spain

O. Almora, C. J. Brabec
Erlangen Graduate School of Advanced Optical Technologies (SAOT)
91052 Erlangen, Germany
E-mail: osbel.almora@fau.de; christoph.brabec@fau.de

D. Baran
King Abdullah University of Science and Technology (KAUST)
Division of Physical Sciences and Engineering (PSE)
KAUST Solar Center (KSC)
Thuwal 23955, Saudi Arabia

G. C. Bazan
Departments of Chemistry and Chemical Engineering
National University of Singapore
Singapore 117543, Singapore

C. I. Cabrera
Unidad Académica de Ciencia y Tecnología de la Luz y la Materia
Universidad Autónoma de Zacatecas
Zacatecas 98160, Mexico

S. Erten-Ela
Solar Energy Institute
Ege University
Bornova, Izmir 35100, Turkey

K. Forberich, J. Hauch, C. J. Brabec
Forschungszentrum Jülich GmbH
Helmholtz-Institut Erlangen-Nürnberg for Renewable Energy (HI ERN)
Institute of Materials for Electronics and Energy Technology (i-MEET)
91058 Erlangen, Germany

F. Guo
Institute of New Energy Technology
College of Information Science and Technology
Jinan University
Guangzhou 510632, P. R. China

A. W. Y. Ho-Baillie
School of Physics and The University of Sydney Nano Institute
The University of Sydney
Sydney, NSW 2006, Australia

T. J. Jacobsson
Institute of Photoelectronic Thin Film Devices and Technology
Key Laboratory of Photoelectronic Thin Film Devices
and Technology of Tianjin
College of Electronic Information and Optical Engineering
Nankai University
Tianjin 300350, P. R. China

since 2020 in the annual emerging PV reports (e-PVr)[1,2] series, of which this is the third version. In this context, not only the performance data of the best e-PV devices (e.g., see Green et al.)[3] are listed, but the values are also put into perspective by comparing the devices in certain categories defined by the class of absorber material or the application. Notably, the e-PVr lists and displays the performance parameters of the top efficiency cells for each technology and at each absorber material bandgap energy and compares the data to the corresponding theoretical limit in the detailed balance (DB)[4–6] model. Additionally, we present the operationally most stable devices as well as the best performing cells in the subcategories of flexible and transparent/semitransparent PVs for single and multiple (now up to three) junction devices.

Similar to previous e-PVr,[2] the criteria for inclusion in these surveys require the data to be published in a peer-reviewed academic journal with a proper "methods" section that allows experimental reproduction of the results as well as basic data to perform self-consistency checks. For the power conversion efficiency (PCE) values, the current density–voltage (J–V) curve

R. A. J. Janssen
Molecular Materials and Nanosystems and Institute
for Complex Molecular Systems
Eindhoven University of Technology
Eindhoven 5600 MB, The Netherlands

R. A. J. Janssen
Dutch Institute for Fundamental Energy Research
De Zaale 20, Eindhoven 5612 AJ, The Netherlands

T. Kirchartz, U. Rau
IEK5-Photovoltaics
Forschungszentrum Jülich
52425 Jülich, Germany

T. Kirchartz
Faculty of Engineering and CENIDE
University of Duisburg-Essen
47057 Duisburg, Germany

N. Kopidakis
PV Cell and Module Performance group
National Renewable Energy Laboratory (NREL)
Golden, CO 80401, USA

M. A. Loi
Photophysics and OptoElectronics Group
Zernike Institute for Advanced Materials
University of Groningen
Nijenborgh 4, Groningen NL-9747 AG, The Netherlands

R. R. Lunt
Department of Chemical Engineering and Materials Science
Department of Physics and Astronomy
Michigan State University
East Lansing, MI 48824, USA

X. Mathew
Instituto de Energías Renovables
Universidad Nacional Autónoma de México
Temixco, Morelos 62580, Mexico

M. D. McGehee
Department of Chemical and Biological Engineering and Materials
Science and Engineering Program
University of Colorado
Boulder, CO 80309, USA

M. D. McGehee
National Renewable Energy Laboratory
15013 Denver West Parkway, Golden, CO 80401, USA

J. Min
The Institute for Advanced Studies
Wuhan University
Wuhan 430072, P. R. China

J. Min
Key Laboratory of Materials Processing and Mold (Zhengzhou University)
Ministry of Education
Zhengzhou 450002, P. R. China

D. B. Mitzi
Department of Mechanical Engineering and Material Science
and Department of Chemistry
Duke University
Durham, NC 27708, USA

M. K. Nazeeruddin
Group for Molecular Engineering and Functional Materials
Ecole Polytechnique Fédérale de Lausanne
Institut des Sciences et Ingénierie Chimiques
Sion CH-1951, Switzerland

J. Nelson
Department of Physics
Imperial College London
London SW7 2BZ, UK

A. F. Nogueira
Chemistry Institute
University of Campinas
PO Box 6154, Campinas, São Paulo 13083-970, Brazil

U. W. Paetzold
Institute of Microstructure Technology (IMT)
Karlsruhe Institute of Technology (KIT)
76344 Eggenstein-Leopoldshafen, Germany

U. W. Paetzold
Light Technology Institute (LTI)
Karlsruhe Institute of Technology (KIT)
76131 Karlsruhe, Germany

B. P. Rand
Department of Electrical Engineering and Andlinger Center for Energy
and the Environment
Princeton University
Princeton, NJ 08544, USA

H. J. Snaith
Clarendon Laboratory
Department of Physics
University of Oxford
Oxford OX1 3PU, UK

E. Unger
Helmholtz-Zentrum Berlin
14109 Berlin, Germany

L. Vaillant-Roca
Photovoltaic Research Laboratory, Institute of Materials Science and
Technology – Physics Faculty
University of Havana
Havana 10400, Cuba

C. Yang
Department of Chemical Engineering and Materials Science
Michigan State University
East Lansing, MI 48824, USA

C. Yang
Solaria Corporation
Fremont, CA 94538, USA

H.-L. Yip
Department of Materials Science and Engineering and Hong Kong
Institute for Clean Energy
City University of Hong Kong
Tat Chee Avenue, Kowloon 999077, Hong Kong

C. J. Brabec
Zernike Institute for Advanced Materials
University of Groningen
Groningen 9747, The Netherlands

measured under standard conditions and the external quantum efficiency (EQE) spectra should be presented and should be consistent insofar that the short-circuit current density (J_{sc}) determined from both methods should not differ by more than 10%. Reporting 5 min of maximum power point (MPP) tracking is encouraged, in particular for perovskite solar cells (PSCs). For flexible and transparent/semitransparent devices, some evidence of the bending radius and the transmittance (T) spectra should be provided, respectively. In the case of operational stability test results, the initial and final efficiencies before and after 200 h or 1000 h are expected to be specified in the published paper. For multijunction devices, from this e-PVr onward we will also include triple junction solar cells, and analogous data of the devices should be provided with particular attention to the material and EQE data of each subcell. In addition, articles lacking some of the mandatory requirements to be included in the e-PVr could be reconsidered, provided a suitable extended or additional supporting document be posted on the emerging-pv.org website. Further details on the accuracy, performance parameters, discarding, and tie rules can be found in the previous e-PVr[1] and in Sections S1.5 and S1.6 of the Supporting Information.

Table 1 summarizes the equations, definitions, and useful references already presented in the previous e-PVr and now updated in the current version, whereas Table S1 of the Supporting Information reviews the minimal details to include in a research article to be considered in an e-PVr. Here we highlight the use of the definition of the photovoltaic bandgap energy as the inflection point of the absorption threshold of the EQE spectrum.[7,8] This definition not only characterizes the operational response of the entire device (rather than an independent absorber layer or set of sublayers), but also provide an unifying framework for comparison between different emerging technologies when a single optical bandgap energy is not directly defined,[1] e.g., in organic photovoltaics (OPVs).

Following the previous e-PVr,[2] each section includes the best performing cells as reported in the literature and grouped in different technologies or material families. The corresponding abbreviations are summarized in **Table 2**. Importantly, for multijunction PV cells we define the top subcell as that which receives the total incident photon flux and generally has the highest absorber material bandgap energy ($E_{g,top}$) in comparison with the other subcell(s). Similarly, the bottom subcell will be the one receiving the last and smaller fraction of the filtered incident photon flux and will generally have the smallest absorber material bandgap energy ($E_{g,bottom}$), in comparison with the other subcell(s). For two junction cells or tandem devices, only the top and bottom subcells are present. Differently, for triple junction cells a middle subcell will be sandwiched in between the top and bottom subcells with an absorber material bandgap energy ($E_{g,mid}$) typically larger than $E_{g,bottom}$ and smaller than $E_{g,top}$.

In this article, the updated graphs and tables of the best performing research photovoltaic cells are presented with the latest reports since August 2021. As an extension of the previous report, single junction AgBiS$_2$-based devices and monolithic/2-terminal triple-junction photovoltaic cells are now incorporated not only among the top efficiency cells but also in the section of flexible photovoltaics. In the plot representations (Sections 2–5), older and newer values are displayed with lighter and darker dot colors, respectively. Similarly, new entries are in a bold case in the tables (see Sections 7.1–7.4, **Tables 3–26**). The following sections not only describe the updated plots and tables resulting from our database but also highlight and discuss the most relevant and recent achievements in each section and comment on general trends and progress in the field during the last year.

Table 1. Equations and definitions considered in this work.

Nos.	Equation	Definitions and comments	Refs.
(1)	$PCE = \dfrac{P_{out}}{P_{in}} = \dfrac{V_{oc} \cdot J_{sc} \cdot FF}{P_{in}}$	PCE, power conversion efficiency; P_{out}, output power density, P_{in}, incoming power density; V_{oc}, open-circuit voltage; J_{sc}, short-circuit current density; FF, fill factor	[1]
(2)	$EQE = \dfrac{A_m}{1 + \exp[\kappa - \dfrac{(\lambda - \dfrac{hc}{E_g})}{\lambda_s}]}$	Procedure to determine E_g from the EQE(λ) spectrum: EQE, external quantum efficiency; λ, wavelength; A_m, maximum EQE value just above the bandgap absorption threshold; h, Planck's constant; c, speed of light; E_g, photovoltaic bandgap energy; λ_s, sigmoid wavelength width parameter (EQE onset quality wavelength), $\kappa = \ln[7 + 4\sqrt{3}] \approx 2.63$, dimensionless coefficient related to the second derivative of the sigmoid.	[7]
(3)	$\dfrac{PCE^{real}}{PCE^{ideal}} = \dfrac{J_{sc}^{real}}{J_{sc}^{ideal}} \dfrac{V_{oc}^{real}}{V_{oc}^{ideal}} \dfrac{FF^{real}}{FF^{ideal}}$	The "real" superscript refers to the experimental values; the "ideal" superscript refers to the theoretical limit of each performance parameter as in the detailed-balance models,[4,5,9] e.g., the highest efficiency for a single junction cell with absorber material of bandgap energy E_g at a temperature T_c under a spectral irradiance Γ.	[10]
(4)	$AVT = \dfrac{\int T(\lambda) P(\lambda) \Gamma_{AM1.5G}(\lambda) d\lambda}{\int P(\lambda) \Gamma_{AM1.5G}(\lambda) d\lambda}$	AVT, average visible transmittance; T, transmittance; P, photopic response of the human eye; $\Gamma_{AM1.5G}$ is the standard 1 sun illumination intensity AM1.5G spectrum, typically in units of W m^{-2} nm^{-1}.	[11]
(5)	$LUE = AVT \cdot PCE$	LUE, light utilization efficiency	[12]
(6)	$E_{\Delta\tau} = \int_0^{\Delta\tau} P_{out} \, dt = \int_0^{\Delta\tau} P_{in} \, PCE \, dt$	$\Delta\tau$, operational stability test time; $E_{\Delta\tau}$, operational stability test energy yield (STEY) for a test of duration $\Delta\tau$; t, time; STEY is taken for 200 and 1000 h of stability tests as E_{200h} and E_{1000h}, respectively.	[1]
(7)	$DR_{\Delta\tau} = \dfrac{PCE(\tau) - PCE(0)}{\Delta\tau}$	$DR_{\Delta\tau}$, effective overall degradation rate for an operational stability test of duration $\Delta\tau$; DR_{200h} and DR_{1000h} are taken as the overall degradation rates for 200 and 1000 h of stability tests, respectively.	[1]

Table 2. Abbreviations for PV technologies or material families considered in this work.

Abbreviation	Meaning and comments
AgBiS	AgBiS$_2$-based single junction photovoltaic cells
a-Si:H	Amorphous silicon single junction photovoltaic cell; for representation purposes, a-SiGe:H-based single junction cells are exceptionally considered within this abbreviation.
CdTe	Cadmium telluride single junction photovoltaic cell
CIGS	CuIn$_x$Ga$_{1-x}$Se$_2$-based single junction photovoltaic cell
CIGS/DSSC	Monolithic/2-terminal tandem photovoltaic cell: CuIn$_x$Ga$_{1-x}$Se$_2$-based bottom subcell and dye sensitized top subcell
CIGS/perovskite	Monolithic/2-terminal tandem photovoltaic cell: CuIn$_x$Ga$_{1-x}$Se$_2$-based bottom subcell and perovskite-based top subcell
CiGS/AlGaAs/GaInP	Monolithic/2-terminal triple junction photovoltaic cell: CuIn$_x$Ga$_{1-x}$Se$_2$-based bottom subcell, AlGaAs-based middle subcell and GaInP-based top subcell
CZTS	Cu$_2$ZnSn(S,Se)$_4$-based single junction photovoltaic cell
DSSC	Dye sensitized single junction photovoltaic cell
DSSC/perovskite	Monolithic/2-terminal tandem photovoltaic cell: dye sensitized bottom subcell and perovskite-based top subcell
GaAs	Gallium arsenide single junction photovoltaic cell
GaAs/GaInP	Monolithic/2-terminal tandem photovoltaic cell: GaAs-based bottom subcell and GaInP-based top subcell
GaAs/perovskite	Monolithic/2-terminal tandem photovoltaic cell: GaAs-based bottom subcell and perovskite-based top subcell
InGaAs/GaAs/InGaP	Monolithic/2-terminal triple junction photovoltaic cell: InGaAs-based bottom subcell, GaAs-based middle subcell, and GaInP-based top subcell
nc-Si/a-Si	Monolithic/2-terminal tandem photovoltaic cell: nanocrystalline or microcrystalline Si bottom subcell and amorphous Si top subcell
nc-Si/nc-Si/a-Si	Monolithic/2-terminal triple junction photovoltaic cell: nanocrystalline silicon-based bottom and middle subcells, and amorphous silicon-based top subcell
OPV	Organic photovoltaic material-based single junction photovoltaic cell
OPV/a-Si	Monolithic/2-terminal tandem photovoltaic cell: organic-based bottom subcell and amorphous silicon-based top subcell
OPV/perovskite	Monolithic/2-terminal tandem photovoltaic cell: the bottom and top subcells are organic- and perovskite-based, respectively or vice versa.
PSC	Perovskite single junction photovoltaic cell
SbS	Sb$_2$(S,Se)$_3$-based single junction photovoltaic cell
Si	Monocrystalline or polycrystalline silicon single junction photovoltaic cell, including homo- or heterojunction structures.
Si/DSSC	Monolithic/2-terminal tandem photovoltaic cell: Si-based bottom subcell and dye sensitized top subcell
Si/GaAsP	Monolithic/2-terminal tandem photovoltaic cell: Si-based bottom subcell and GaAs$_{1-x}$P$_x$-based top subcell
Si/GaInAsP/InGaP	Monolithic/2-terminal triple junction photovoltaic cell: silicon-based bottom subcell, GaInAsP-based middle subcell, and GaInP-based top subcell
Si/perov/perov	Monolithic/2-terminal triple junction photovoltaic cell: Si-based bottom subcell and perovskite-based middle and top subcells
Si/perovskite	Monolithic/2-terminal tandem photovoltaic cell: Si-based bottom subcell and perovskite-based top subcell
TLSC	Transparent luminescent solar concentrator, including a lightguide, luminophore, and mounted solar cell(s).

2. Highest Efficiency Research Photovoltaic Cells

2.1. Single Junction Devices

The top efficiency single junction research cells are summarized in **Figure 1** as a function of the PV bandgap, along with the detailed-balance theoretical efficiency limit[4] for a single junction assuming radiative emission from the front and the rear side of the photovoltaic cell.[13] The new entries in the database are highlighted in more opaque colors.

Overall, most of the new record cells belong to the group of PSCs and OPVs. The compositional space of the perovskite absorber materials is large and the new reports are scattered over nearly all the bandgap range of Figure 1. On the other hand, the OPVs seem to cluster in the range 1.39–1.42 eV, apparently due to the commonly employed polymer PM6 included in many binary and ternary blends used as active layers in these

cells. It can be seen that PSCs outperform OPVs, and all other new entries for e-PVs, in terms of V_{oc} and FF and hence also in PCE. Importantly, new records were reported for dye-sensitized,[14] kesterite,[3] and antimony selenosulfide[15] devices and the AgBiS$_2$-based cells are now included as a new technology in our plots. Moreover, some other new reports have been added for crystalline-silicon based heterojunction[16] solar cells, which are still below the top efficiency reported cells for their respective technologies.

Among new PSCs entries, the new absolute certified record with an efficiency of 25.7% was reported in the tables published by Green et al.,[3] which does not include further information beyond the performance parameters and the EQE spectrum. A similar 25.7% efficiency (25.4% certified) was reported by Kim et al.[17] for a FAPbI$_3$-based device where the commonly used mesoporous–titanium dioxide electron transport layer was replaced with a thin layer of polyacrylic acid–stabilized tin(IV)

**ADVANCED
SCIENCE NEWS**

www.advancedsciencenews.com
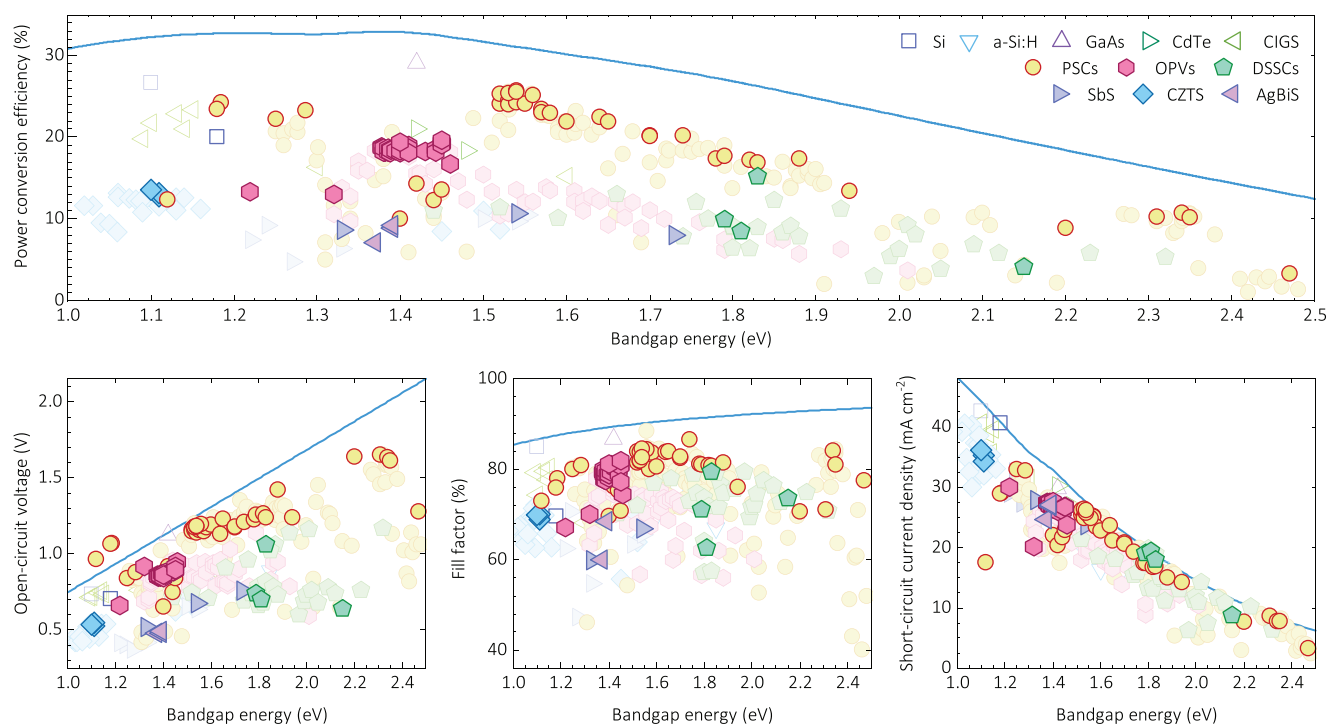
**ADVANCED
ENERGY
MATERIALS**

www.advenergymat.de

Figure 1. Highest efficiency single junction photovoltaic cells. Performance parameters as a function of effective absorber bandgap for different photovoltaic technologies: power conversion efficiency (top) open-circuit voltage (bottom left), fill factor (bottom center), and short-circuit current density (bottom right). Experimental data are summarized in Section 7.1, with the lighter and opaquer dots corresponding to the older and updated cells, respectively. The solid lines indicate the corresponding theoretical detailed-balance efficiency limit.[13]

oxide quantum dots (paa-QD-SnO$_2$) on the compact titanium dioxide. This strategy not only proved to increase efficiency but also stability and potential for scalability, achieving over 20% efficiency for a 64 cm^2 solar minimodule. Moreover, Zhao et al. presented another FAPbI$_3$-based cell with a certified efficiency of 25.6%. In this case, the authors stabilized the perovskite phase by converting the secondary-phase excess lead iodide (PbI$_2$) into an inactive (PbI$_2$)$_2$RbCl compound via doping with rubidium chloride (RbCl).

Additional notable developments in the field of opaque, single junction perovskite solar cells are significant improvements in fill factor. While the fill factor of halide perovskites with typical bandgaps in the range ≈1.6 eV could exceed 90% in the detailed balance limit, in practice reported fill factors were mostly in the range of 80% to 84% for the best devices.[18] Recently, however, strategies based on interface modifications were reported to improve the fill factor up to 86% even for areas >1 cm^2 while at the same time enabling high efficiencies above 23%.[19] Also in the field of higher bandgap p–i–n type perovskite solar cells, high fill factors above 86% were achieved by interfacial passivation with guanidinium bromide.[20]

A second development in the last year was that the device geometry that is alternatively called p–i–n type or inverted geometry was making significant improvements in peak efficiency, thereby closing the gap toward n–i–p type or regular geometry perovskites. Again, interfacial passivation enabled the first >25% p–i–n type perovskite solar cells as reported by Li et al.[21] whereas the current top efficiency for this device design was achieved by Jian et al.[22] with a 25.3% (24.1%

certified) cell. The latter work proposed a reactive surface engineering approach based on a postgrowth treatment of 3-(aminomethyl)pyridine (3-APy) on top of the perovskite thin film, which not only resulted in increased efficiency but also in operational stability over >2000 h (see also Section 5).

Intriguingly, at least two articles[23,24] about Sn-based PSCs report device structures that apparently fit the traditional definition of single junction cells but result in anomalously high V_{oc} values, even above the corresponding radiative DB limits (see Figure 1 bottom-left). Besides the relatively low E_g values, these cells have in common the complexity of the absorption layer(s) toward the electron transport layer (ETL). Specifically, Zhou et al.[24] included a BTBTI:PCBM blend in between the perovskite and the ETL, whereas Lei et al.[23] introduced low-dimensional Bi^{3+}-alloyed BA$_2$MA$_4$Sn$_5$I$_{16}$ superlattices by chemical epitaxy. Although none of the works provided major justifications for these behaviors, one may hypothesize that mobilities and lifetimes significantly change as a function of depth thereby invalidating the assumption of flat quasi-Fermi levels (at open-circuit) typically used to calculate the radiative limit of V_{oc}. Importantly, while this effect could lead to V_{oc} values above the DB limit, it cannot lead to PCE values above the DB limit.

For OPVs, a consolidated set of at least 25 reports with cells having over-18% efficiency illustrates the significant progress during the last year. The highest efficiency entries are the 19.6% (19.2% certified) efficient solar cell reported by Zhu et al.[25] and the 19.05% of Wei et al.[26] For the highest efficiency, the focus was on the morphology optimization of the ternary blend PM6:D18:L8-BO, while the approach of Wei et al. centered on
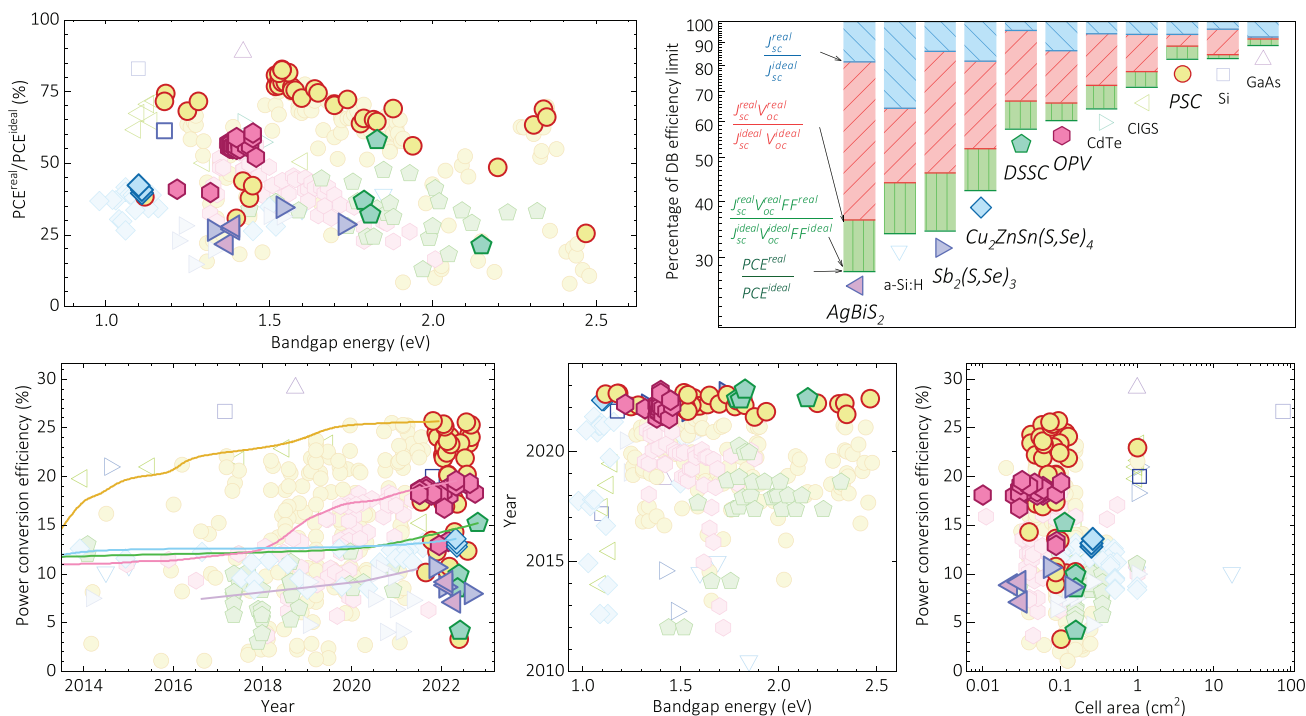
Figure 2. Analysis of PCE data in Figure 1 with respect to the DB efficiency limit (top panel), the publication date (bottom-left and -center) and the device or active area of the record cells (bottom-right). The top-left graph shows the relative efficiencies with respect to the theoretical limit for all the cells and the top-right graph presents the logarithmic loss analysis for the top efficiency cell of each technology, as defined by Equation (3) of Table 1. The legend is as that of Figure 1, where opaque and light symbols indicate recent and older reports, respectively. The solid lines in the bottom-left graph contain the data from NREL's "Best research-cell efficiency chart.[33]

the sequential deposition of the binary blend D18:L8-BO. Moreover, another interesting result by Liu et al.[27] is highlighted in terms of the development of low-bandgap OPVs, which achieved a 13.35% efficiency solar cell based on the binary blend PTB7-Th:ATT-9 with a photovoltaic bandgap of 1.22 eV. This result not only allowed a remarkable photocurrent of 30 mA cm^{-2} for application in semitransparent photovoltaics but also shows potential for integration into multijunction devices as rear subcell.

The latest record performance Cu$_2$ZnSn(S,Se)$_4$ cell has been reported by Green et al.[3] with a certified efficiency of 13.6%. More recently, Wang et al.[28] showed a 13.14% (12.8% certified) efficiency device resulting from introducing a thin GeO$_2$ layer on Mo substrates. This strategy was suggested to produce a bidirectional diffusion of Ge, which reduced the defect density and thus the V_{oc} deficit.

Another new efficiency record has been reported among Sb$_2$(S,Se)$_3$ solar cells from a device reported by Zhao et al.[15] with a PCE of 10.7%. Here, alkali metal fluorides post treatments are applied to improve the quality of Sb$_2$(S,Se)$_3$ films by manipulating the S/Se gradient in the films, which creates a favorable energy alignment for the charge carrier transport. Notably, although earlier proposed as all-inorganic devices,[29] it has only been after the inclusion of spiro-OMeTAD as a hole selective layer SbS cells[15,30,31] that the efficiencies exceeded 10%.

The new introduction to our graphs and tables for single-junction devices are photovoltaic cells based on AgBiS$_2$

absorbers. The current champion cell presents a 9.17% (8.85% certified) efficiency, as reported by Wang et al.[32] who found that cation-disorder-engineered AgBiS$_2$ colloidal nanocrystals optimize the absorption coefficient. This enabled 30 nm thick absorber photovoltaic devices for a remarkable photocurrent of 27 mA cm^{-2}.

Most recently, a new record efficiency for DSSCs was reported by Ren et al. with a certified PCE value of 15.2%. Their result was possible with cells that included a monolayer of a hydroxamic acid derivative on the surface of TiO$_2$ to improve the dye molecular packing and overall photovoltaic performance of two newly designed coadsorbed sensitizers: SL9 and SL10. These cosensitized devices not only achieve remarkable performance among the entire family of DSSCs, but also exhibit a relative optimization level comparable to top efficiency OPV and wide bandgap PSCs. The latter is illustrated in Figure 1 where the new record DSSC outperforms OPVs in terms of V_{oc} and shows similar values of FF. A similar conclusion is also evident when considering the DB efficiency limits for the corresponding E_g, as presented in **Figure 2**.

The analyses on the current state-of-the-art device performance with respect to the DB efficiency limit are illustrated in an alternative way in the top panel of Figure 2. In the top-left plot of that figure one can find the same efficiency data as in Figure 1, but now in terms of the ratio between the experimental value and the theoretical limit for the efficiency, as defined in Equation (3) of Table 1. Of emerging devices, PSCs

**ADVANCED
SCIENCE NEWS**

www.advancedsciencenews.com

**ADVANCED
ENERGY
MATERIALS**

www.advenergymat.de
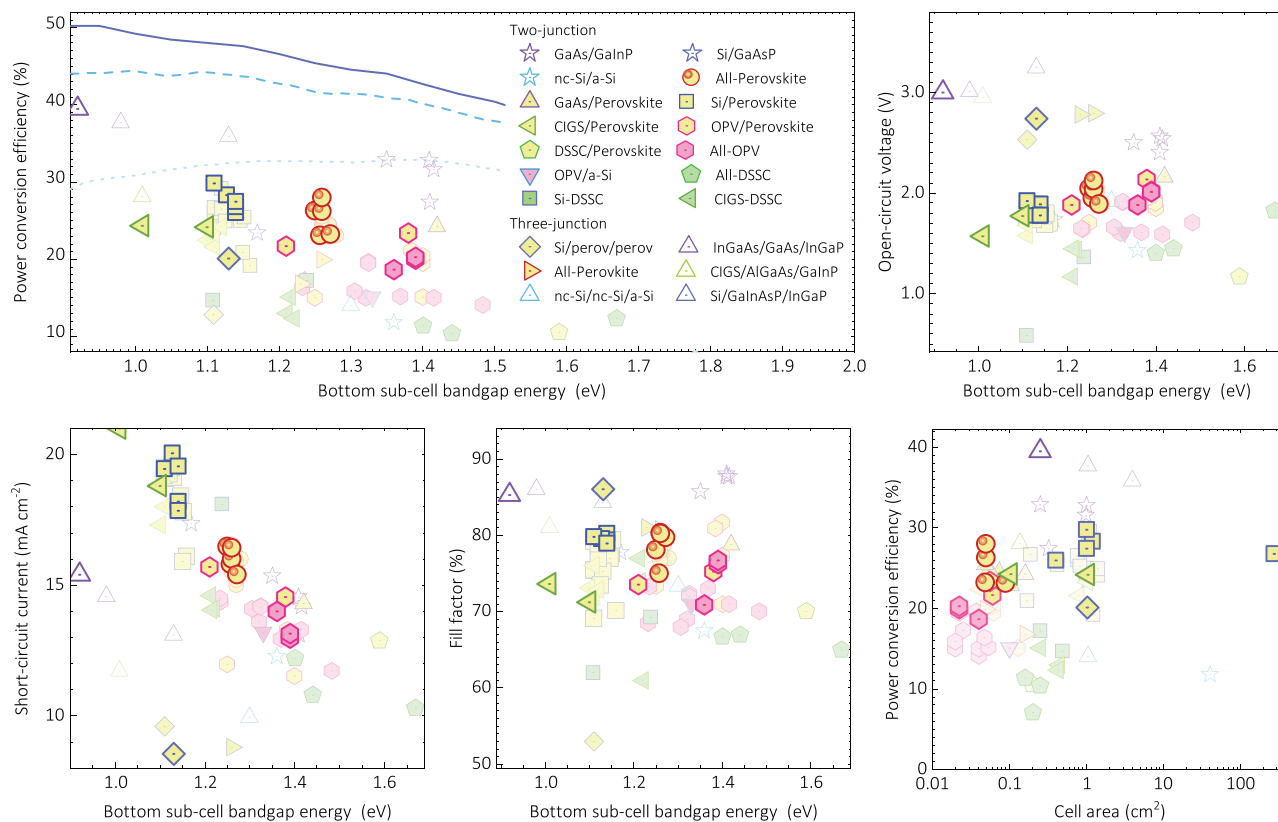
Figure 3. Highest efficiency for monolithic/two-terminal multijunction photovoltaic research cells including up to three junctions. Performance parameters as a function of the absorber bandgap energy of the bottom subcell for various photovoltaic technologies: power conversion efficiency (top-left), open-circuit voltage (top-right), short-circuit current density (bottom-left), fill factor (bottom-center), and corresponding area (bottom-right). The dotted, dashed, and solid lines in the efficiency graph indicate the single junction, the top-subcell-optimized and top- and middle-subcell-optimized DB efficiency limits for one junction, double junction, and triple junction photovoltaic cells, respectively.[5,9] Light and opaque dots indicate the reports published before and after August 2021, respectively.

exhibit the highest degree of optimization, up to 82% of the DB limit, which is only outperformed by silicon and GaAs single junction cells. Even the wide-bandgap (≈2.34 eV) PSCs can achieve 69% of the theoretical limit, while all other e-PV technologies are below 60%. Furthermore, the top-right graph in Figure 2 shows the loss analysis for the champion efficiency cells of each technology, highlighting with bold labels and opaque symbols the new entries in the current e-PVr. The new top efficiency PSC[3] not only matches the relative performance of the silicon solar cell but also shows a nearly even distribution of losses between photovoltage, photocurrent and FF. By contrast, the five other new record cells (DSSC,[14] OPV,[25] CZTS,[3] Sb$_2$Se$_3$,[15] AgBiS$_2$)[32] show the persistent[2] major influence of photovoltage losses over any other parameter.

The time evolution of the device performance presented in Figure 1 is shown in detail for the bottom-left and -center graphs of Figure 2. Among e-PV technologies, the evolution of the efficiency since 2010 evidences the apparent saturation and/or stagnation for the performance optimization of PSCs, DSSCs, CZTS, and Sb$_2$Se$_3$ solar cells, as presented in the bottom-left graph of Figure 2, which also includes the

data from NREL's "Best research-cell efficiency chart" (solid lines).[33] Notably, OPV devices display an apparent upswing with significant improvement in efficiency during the last year. The time evolution of material variability within technologies is illustrated in the bottom-center graph of Figure 2. Notably, the research on OPV seems to have gradually lost interest in active materials whose effective photovoltaic bandgap exceeds 1.5 eV. Even though this is related to the emergence of non-fullerene acceptors and the latest increase in efficiency, the lack of progress in the wide-bandgap OPVs may limit progress of all-organic multijunction solar cells.

Regarding scalability, the PCE values as a function of the cell area are now included for rigid and flexible cells in **Figures 2–4**. Notably, the accuracy and type of area (see, e.g., Green et al.[34]) are not specified due to the irregular and often poor description of this parameter in the literature. Therefore, the current version of our plots is focused on indicating the order of magnitude of the cell area rather than specific values, which can be easier to find at emerging-pv.org. Moreover, we highlight that only cells are examined. Although the analysis of PV modules may be interesting for future versions of the e-PVr, the design
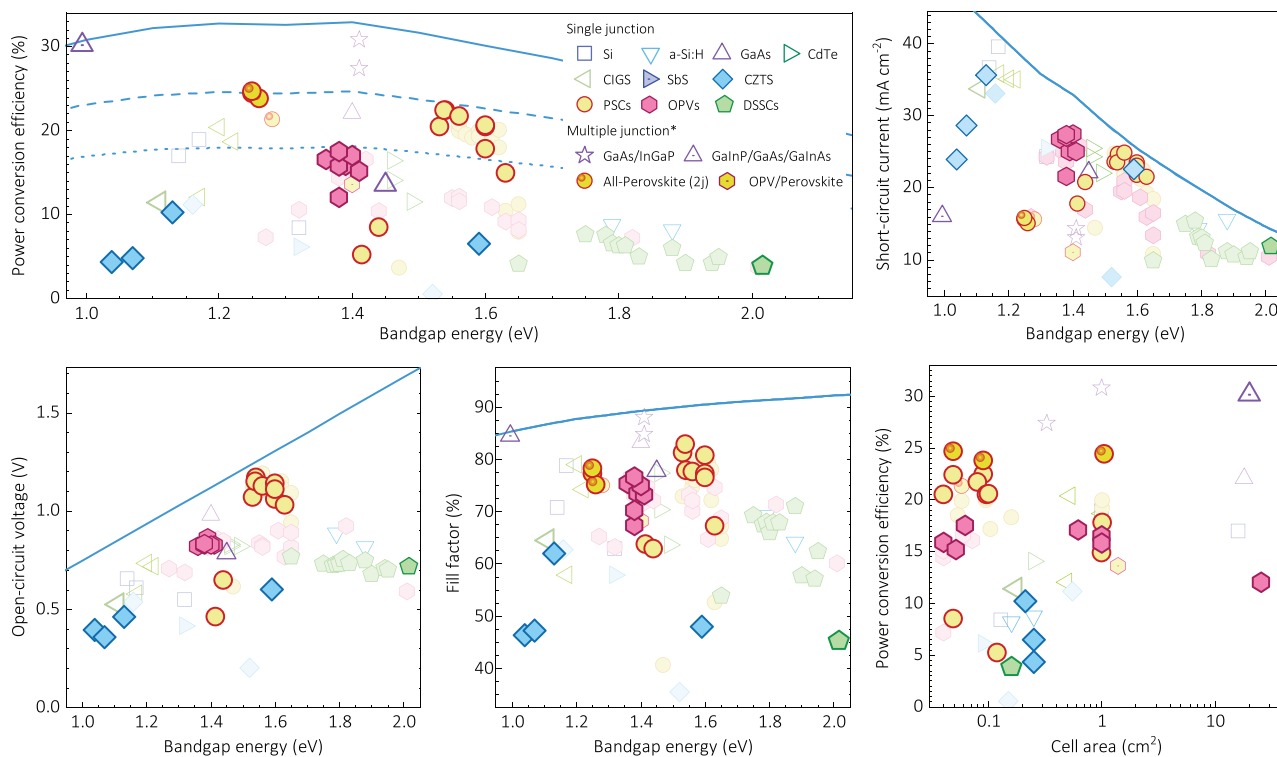
Figure 4. Flexible PVs and their performance parameters as a function of absorber (or bottom junction absorber in case of multijunction devices) bandgap energy for various photovoltaic technologies: power conversion efficiency (top-left), short-circuit current density (top-right), open-circuit voltage (bottom-left), fill factor (bottom-center), and efficiency versus area (bottom-right). Experimental data are summarized in Section 7.2 and the solid, dashed, and dotted lines indicate 100%, 75%, and 55% of the theoretical single junction DB efficiency limit,[13] respectively.

differences of these devices and the volume of data to process may require a separated section, which lies beyond the scope of the present survey.

From the efficiency-area data for the single junction cells in Figure 2, e-PV technologies are still significantly behind established PV technologies, such as silicon and CIGS. Most of the new record performance cells among PSCs, OPVs, and AgBiS$_2$-based devices do not exceed 0.1 cm^2, and DSSCs, CZTS, and SbS cells are just slightly larger but still smaller than 0.5 cm^2. Markedly, Peng et al.[19] reported a certified efficiency of 22.97% for a 1 cm^2 PSC where the electron transport layer was optimized by a reverse-doping process to fabricate nitrogen-doped titanium oxide. This strategy was suggested to reduce electrical series resistance in favor of FF enhancement.

2.2. Multijunction Devices (Monolithic)

The performance parameters of monolithic/two-terminal multijunction photovoltaic research cells with up to three junctions are presented in Figure 3 and are put into perspective by comparison to the corresponding optimized bandgap DB efficiency limit including radiative coupling. Overall, multijunction e-PV devices continue to show smaller efficiencies in comparison with established technologies (e.g., GaAs/GaInP, Si/GaInAsP/InGaP) and even with respect to the single junction

DB efficiency limit corresponding to their bottom-subcell bandgap energy (dotted line in the top-left graph of Figure 3). The most significant progress during the last year is among Si/perovskite and all-perovskite tandem solar cells with top certified efficiencies of 29.8% and 28%, as respectively reported by Green et al.,[3] and at least one more cell for each technology has attained efficiencies over 26%. These devices present similar values of V_{oc} and FF among themselves, and in comparison with OPV/perovskite and all-OPV tandem cells. Yet, the superior photocurrent of Si/perovskite and all-perovskite tandem cells is the reason they outperform the other e-PV technologies. With regard to perovskite/CIGS tandem solar cells the development of new bandgap combinations, using narrow-bandgap (≈1.01 eV) gallium-free CIS bottom cells, lead to good performance of 23.5% certified.[35] In terms of scalability (see bottom-right plot of Figure 3), only the new cells of Si/perovskite and CIGS/perovskite show promising areas equal/close to 1 cm^2, whereas all other devices were tested with areas smaller than 0.1 cm^2.

Among the champion cells, to start with, we highlight the all-perovskite double junction cell by Lin et al.[36] who reported a certified efficiency of 26.3%, a value that exceeds 25.7% of the top efficiency single junction PSC.[3] Their achievement was based on the development of ammonium-cation-passivated Pb–Sn perovskites with long diffusion lengths, by adding a small amount of 4-trifluoromethyl-phenylammonium (CF$_3$-PA) into

**ADVANCED
SCIENCE NEWS**

www.advancedsciencenews.com

**ADVANCED
ENERGY
MATERIALS**

www.advenergymat.de

the precursor solution. The use of this additive increased not only efficiency but also stability.

A Si/perovskite tandem device with 28.84% (28.34% certified) efficiency for a device area of 1.2 cm^2 has been reported by Mao et al.[37] In their study, they optimized the interface between the silicon and the perovskite subcells by developing a NiO$_x$/2PACz ([2-(9H-carbazol-9-yl) ethyl]phosphonic acid) ultrathin hybrid hole transport layer above the ITO. The NiO$_x$ interlayer facilitates a uniform self-assembly of 2PACz molecules onto the fully textured surface, thus avoiding direct contact between ITO and perovskite top-cell for a minimal shunt loss. This approach not only enables highly efficient tandem cells with industrial compatible silicon bottom cells, but also provides an effective substitute for the specially prepared tunnel junctions.

The first-ever monolithic CIS/perovskite tandem solar cell has been reported by Ruiz-Preciado et al.[35] with a PCE exceeding 23% (23.5% certified, area: 0.5 cm^2). The relatively planar surface profile and narrow bandgap of the CIS bottom subcell allowed them to deposit perovskite top subcells of lower bandgap and with a smaller amount of bromide content, which is desirable to reduce photodegradation.

The triple junction cells show no significant progress in terms of device performance during the last year. For Si/perov/perov and all-perovskite devices, the top efficiencies are still 20.1%[38] and 19.9%,[39] which are significantly smaller in comparison with most of the perovskite-based single and double junction devices. On the other hand, the latest record of GaInP/GaAs/GaInAs photovoltaic cell with a 39.5% efficiency reported by France et al.[40] is the highest efficiency considered in this survey. The key strategy for obtaining this result was the modification of the middle subcell bandgap by using thick GaInAs/GaAsP strain-balanced quantum wells for improved photovoltage and absorption.

3. Flexible Photovoltaic Cells

The research on flexible PVs has shown significant activity during the last year, resulting in several new-record-cell reports for almost all the e-PV technologies, as summarized in Figure 4. In general, flexible single junction PSCs and all-perovskite tandem devices present the highest efficiencies (≈75% of the DB limit) with comparably high FF values. Further, flexible OPV shows consolidated progress not only in efficiency (≈55% of the DB limit), but also in scalability with at least one report over 20 cm^2. With the lowest performances, new reports of kesterite and dye-sensitized solar cells are below or in the efficiency range of 10%.

Among the most remarkable results, Li et al.[41] presented a flexible all-perovskite tandem cell with an efficiency of 24.7% (certified as 24.2%) that retains its initial performance after 10 000 cycles of bending at a radius of 15 mm. Such an achievement was possible thanks to the use of a mixture of two hole-selective molecules based on carbazole cores and phosphonic acid anchoring groups to form a self-assembled monolayer that connects the perovskite with a low temperature-processed NiO nanocrystal film. With this approach, the hole-selective contact is suggested to mitigate interfacial recombination and facilitate hole extraction.

Notably, Zeng et al.[42] fabricated not only a 6 mm^2-device with the highest efficiency among flexible OPVs (17.5%), but also a 1 cm^2 cell with a PCE = 15.82%. In their study, an ionic liquid-type reducing agent containing Cl$^-$ and a dihydroxyl group was employed to control the reduction process of silver in silver-nanowire-based flexible transparent electrodes. This strategy was suggested to decrease the sheet resistance and enhance the mechanical stability of the flexible transparent electrodes. Regarding the flexibility test, the small-area device could retain 82.5% of its initial PCE after 6000 bending cycles, at a bending radius of 4 mm, and 86.1% after 1200 bending cycles of complete folding (bending radius of 0 mm). Furthermore, the 1-cm^2 device retained 78% of its initial PCE values after 6000 bending cycles, at a bending radius of 4 mm.

Flexible triple junction devices based on emerging technologies have not been included in the present survey. On the other hand, we highlight the exceptional results from Schön et al.,[43] who optimized a Ga$_{0.73}$In$_{0.27}$As/GaAs/Ga$_{0.51}$In$_{0.49}$P device grown on 10 µm-thick GaAs substrates for an efficiency of 30.19% under AM0 with 20 cm^2. Furthermore, a mass density of only 13.2 mg cm^{-2} leads to a remarkable power-to-mass ratio of 3.0 W g^{-1}.

4. Transparent and Semitransparent Photovoltaic Cells

Transparency continues to be an import metric, with several key/notable developments. Yet, as defined by our inclusion criteria, the amount and values of the reports in this e-PVr have decreased with respect to the previous version. **Figure 5** illustrates the main performance parameters for each new record cell as a function of the average visible transmittance and the bandgap energy. Overall, most of the new reports come from OPVs, which is over the same amount of those of PSCs and DSSCs combined. No significant progress is reported for the light utilization efficiency and the significant gap in V_{oc} continues to be the main feature distinguishing the performance between PSCs and the other e-PV technologies.

Remarkably, Liu et al.[44] reported an OPV device with average visible transmittance (AVT) = 46.79% and a PCE = 11.44% for a light utilization efficiency (LUE) = 5.35%, which currently is the highest LUE value in our lists. The fabricated cell included a new design for the transparent rear electrode via integrating an aperiodic band-pass filter of [lithium fluoride [LiF]/tellurium dioxide[TeO$_2$]]^8/LiF produced by thermal evaporation. In addition, a systematic optimization of the composition ratio and thickness of the active layer of PM6:BTP-eC9:L8-BO was also required.

Among PSCs, we also highlight the work by Yu et al.[45] who fabricated a semitransparent cell with AVT = 35% and PCE = 12% for an LUE = 4.2%. This is the second and third highest value of LUE among new reports in this survey and all-times reports for PSCs, respectively. Their optimization approach was based on tuning the perovskite composition consisting of cesium (Cs) and formamidinium (FA), which they suggest to produce the best device performance over a range of bandgaps. Furthermore, their CsFA-based semitransparent PSCs show
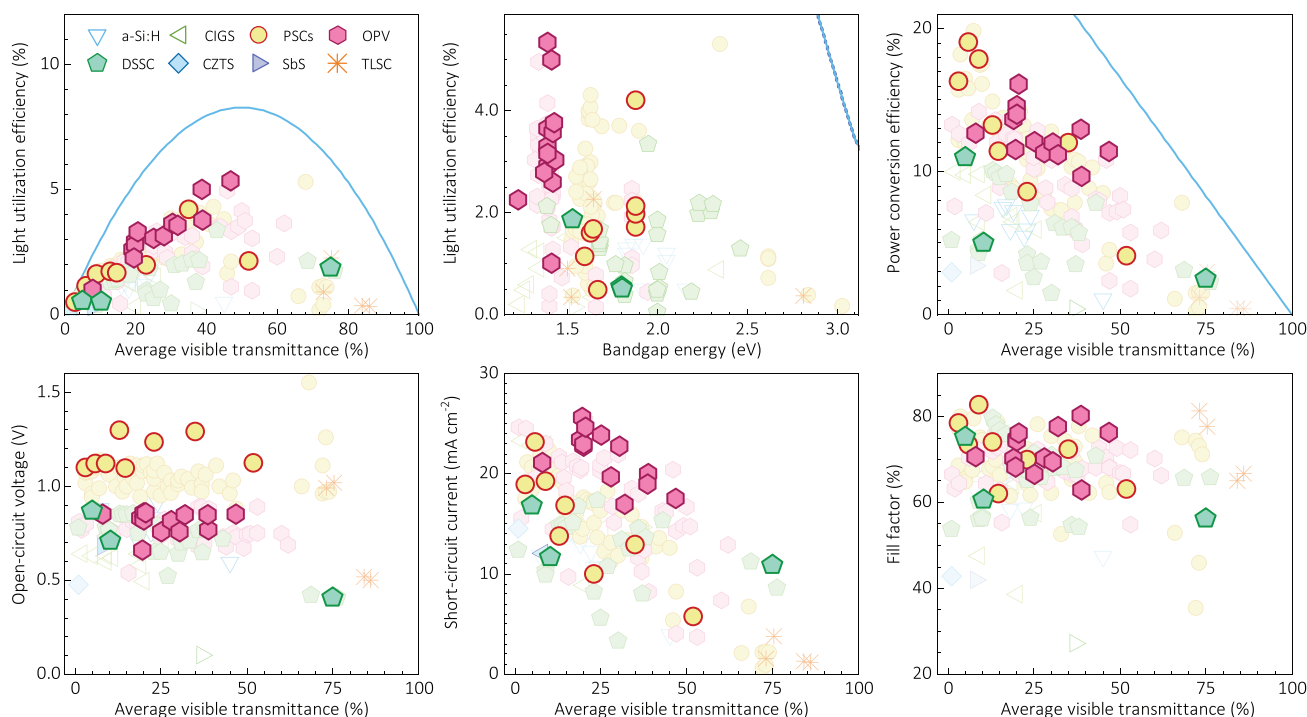
Figure 5. Best performing transparent and semitransparent PVs: light utilization efficiency versus average visible transmittance (top-left) and photovoltaic bandgap energy (top-center); and power conversion efficiency (top-right), open-circuit voltage (bottom-left), short-circuit current density (bottom-center), and fill factor (bottom-right) as a function of average visible transmittance. Experimental data are summarized in Section 7.3. The blue solid lines indicate the corresponding theoretical detailed balance efficiency limit for non-wavelength selective PVs.

improved long-term stability under continuous illumination and heating.

Achieving the highest AVTs can be challenging in thin film PV devices due to optical losses of the transparent electrodes and other functional layers. With an absence of electrodes over the collection area, transparent luminescent solar concentrators (TLSCs) can effectively overcome this challenge. Table 22 summarizes the performance parameters of the devices with TLSCs that report the highest photovoltaic efficiencies, measured in agreement with the standard procedure of Yang et al.[46,47] Note that our list only includes reports published until early 2021, since more recent works in the literature focus on the material and optical properties of the TLSC over the entire photovoltaic device characterization. Nevertheless, we highlight the work by Yang et al.[48] that demonstrated TLSCs with massive-downshifting phosphorescent nanoclusters and fluorescent organic molecules as ultraviolet and near-infrared selective-harvesting luminophores. The design and optimization resulted in dual-band TLSC exhibiting a record PCE = 3.0% with and an AVT = 75% (i.e., LUE of 2.36%) and another champion TLSC with LUE of 2.61% (PCE = 3.65% with a slightly lower AVT = 71.6%) with large device active area of 25.8 cm². Notably, these transparent solar cells are the highest LUE reported for AVT > 70 for any technology (OPV, DSSC, or PSC), and demonstrate a wavelength-selective transparent photovoltaic device exceeding the non-wavelength-selective practical limit (at high AVT).

5. Operational Stability in Emerging Research Solar Cells

Operational stability of e-PV technologies not only continues to be the "Achilles' heel" in the development of these photovoltaic devices, but also arguably the most irregularly documented and tackled research subject in the field. **Figure 6** summarizes the latest reports with in situ 200 and 1000 h stability tests under continuous illumination, in agreement with our inclusion criteria. The latest data relate to single and double-junction perovskite-based devices. Notably, even though the new report for the stability of the all-perovskite tandem cell attains the highest energy yield (left panel in Figure 6), due to the 25.6% of initial PCE (central panel in Figure 6), its overall degradation rate (right panel in Figure 6) is one of the lowest (largest absolute) values in this report. This reinforces the general trend already identified in our previous e-PVr for the multijunction perovskite-based devices to present lower stability than single junction cells.

Also worth mentioning, Sanchez-Diaz et al.[49] not only fabricated and measured the device with the smallest degradation rates (DR$_{200h}$ = 0.006% per day and DR$_{1000h}$ = 0.02% per week) in this report, but also did it for a lead-free PSCs with a significantly high initial efficiency of 9.4%. Their achievement was possible thanks to the addition of dipropylammonium iodide (DipI) together with sodium borohydride (NaBH$_4$) as a reducing agent for preventing the premature degradation of

**ADVANCED
SCIENCE NEWS**

www.advancedsciencenews.com

**ADVANCED
ENERGY
MATERIALS**

www.advenergymat.de

the tin-based perovskite. For the entire stability test, the cell was kept at maximum power point and the cell was at 96% of the initial PCE after 1300 h under simulated 1 sun illumination in N₂.

6. Conclusions

In summary, the third version of the emerging-PV reports presents a substantial data update to the landscape of achievements in the field of PV research. Among the most significant and positive trends, we have evidenced the boom in PCE increase of OPVs and the continuous progress of the perovskite-based tandem solar cells. Further new record performance reports have occurred among single junction PSCs, with special interest among lead-free devices.

Negatively, no significant recent progress has been found among triple junction e-PV technologies and the overall field of transparent and semitransparent PVs. Similarly, but reinforcing a previously known trend, the studies on performance stability continue to be scarce and/or poorly described, which hinders the analysis and comparison of the results within the literature. On the latter, we repeatedly encourage the PV research community to use dimensional and performance-limit-normalized parameters (e.g., $DR_{\Delta \tau}$, $E_{\Delta \tau}$) rather than, or in addition to, relative percentages in the degradation and optimization studies.

7. Tables

The tables below list the reports on best achievements in most of the established and emerging PV technologies as a function of the device bandgap E_g. Unless noted, the E_g values were estimated by fitting the absorption threshold region of the corresponding EQE spectra to Equation (2) of Table 1. Note that, for some absorber materials this definition may result in a value slightly larger (typically on the order of the thermal energy) than that of the optical bandgap.[6] The new reports, from articles published since August 2021, are highlighted in bold. The older reports, from articles published since August 2021, which were already included in our previous surveys are referenced to the corresponding ePVr. By contrast, each older report that was missed in the corresponding previous e-PVr, is now included with its corresponding individual citation. All the citations and further data and visualization tools can be found at the emerging-pv.org website.

In the case of PCE reports of PSCs showing hysteresis behavior in the J–V characteristic, while sweeping voltage in different directions and/or scan rates, the lower PCE value has been considered in each case. Further details are in Section S1.1 of the Supporting Information.

The FF values have been automatically corrected to match the reported values of PCE, J_{sc}, and V_{oc} under standard 100 mW cm⁻² illumination of AM1.5G spectrum. For some reports, this has introduced up to ±0.5% discrepancies
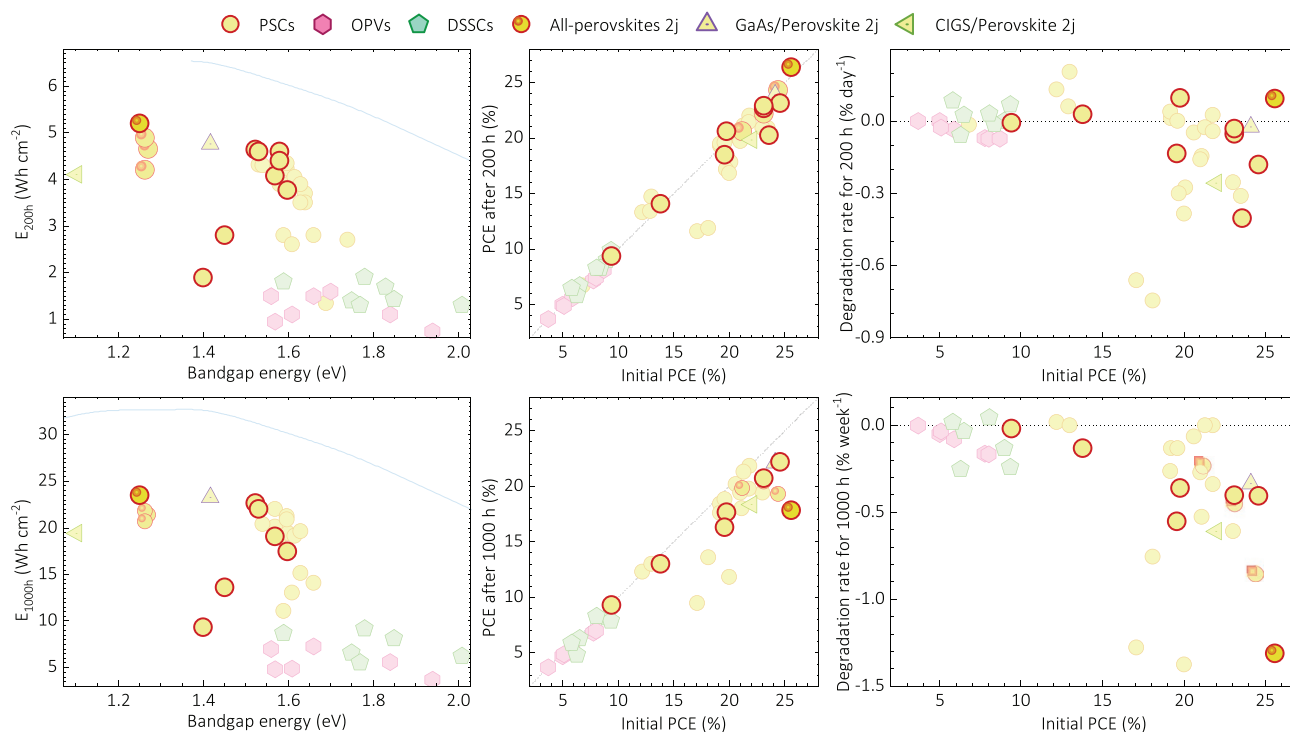
Figure 6. Operationally most stable emerging PVs for each technology during 200 h (top) and 1000 h (bottom) of testing: stability test energy yield (Equation (6) of Table 1) as a function of bandgap energy (left), final power conversion efficiency as a function of the initial value (center), and overall degradation rate (Equation (7) of Table 1) as a function of initial power conversion efficiency (right). The experimental data are summarized in Section 7.4 and the solid blue lines in the STEY panel (left) are the corresponding DB theoretical limits. The diagonal dot-dot-dashed lines in the middle panel indicate where the final efficiencies equal the initial values. The positive values above the horizontal dotted lines in the degradation rate panel (right) indicates that PCE increases with respect to the initial values.

between the values in our tables and those informed in the original publications due to differences in the rounding digits and/or typos in the original manuscripts. Cells with mismatches >0.5% may have been discarded (see Section S1.5, Supporting Information).

For the transparent/semitransparent cells, note that the AVT values may differ from those reported in the original manuscripts when a definition different than that of Equation (4) in Table 1 was used in the original published article.

7.1. Highest Efficiency Research Solar Cells Tables

Tables 3–10 summarize the experimental data of the highest efficiency research solar cells.

Table 3. Single junction perovskite research solar cells with the highest efficiency: performance parameters as a function of device absorber bandgap energy (from EQE spectrum).

E_g [eV]	PCE [%]	V_{oc} [mV]	J_{sc} [mA cm^{-2}]	FF [%]	Absorber perovskite	Refs.
1.12	**12.4**	**967**	**17.5**	**72.9**	**MAPb$_{0.5}$Sn$_{0.5}$Br$_3$:Bi^{3+}:BA$_2$MA$_4$Sn$_5$I$_{16}$**	[23]
1.18	**24.3**	**1070**	**29.1**	**78.0**	**FA$_{0.7}$MA$_{0.3}$Pb$_{0.7}$Sn$_{0.3}$I$_3$/BTBTI:PCBM**	[24]
1.18	23.4	1067	28.9	75.8	FA$_{0.7}$MA$_{0.3}$Pb$_{0.7}$Sn$_{0.3}$I$_3$/BTBTI:PCBM	[24]a)
1.25	20.7	843	30.6	80.2	FA$_{0.6}$MA$_{0.4}$Pb$_{0.4}$Sn$_{0.6}$I$_3$	[2]
1.25	**22.2**	**841**	**33.0**	**80.0**	**FA$_{0.7}$MA$_{0.3}$Pb$_{0.5}$Sn$_{0.5}$I$_3$**	[36]
1.26	20.4	834	30.5	80.2	GuaSCN:FA$_{0.6}$ MA$_{0.4}$Sn$_{0.6}$Pb$_{0.4}$I$_3$	[2]
1.27	20.9	827	31.4	80.5	FA$_{0.7}$MA$_{0.3}$Pb$_{0.5}$Sn$_{0.5}$I$_3$	[2]
1.28	20.6	842	30.6	80.1	FSA: FA$_{0.7}$MA$_{0.3}$Pb$_{0.5}$Sn$_{0.5}$I$_3$	[2]a)
1.28	21.7	850	31.6	80.8	FSA: FA$_{0.7}$MA$_{0.3}$Pb$_{0.5}$Sn$_{0.5}$I$_3$	[2]
1.29	**23.3**	**880**	**32.8**	**80.8**	**Cs$_{0.025}$FA$_{0.475}$MA$_{0.5}$Pb$_{0.5}$Sn$_{0.5}$I$_{2.925}$Br$_{0.075}$**	[50]
1.30	18.8	820	29.6	77.3	FA$_{0.6}$MA$_{0.4}$Pb$_{0.4}$Sn$_{0.6}$I$_3$	[2]
1.30	17.1	840	27.9	73.0	Cs$_{0.05}$FA$_{0.8}$MA$_{0.15}$Pb$_{0.5}$Sn$_{0.5}$I$_3$	[2]
1.31	5.0	420	23.8	50.3	CsSnI$_3$	[2]c)
1.31	7.1	486	22.9	64.0	MASnI$_3$	[2]c)
1.31	14.1	740	26.7	71.4	Cs$_{0.25}$FA$_{0.75}$Pb$_{0.5}$ Sn$_{0.5}$I$_3$	[2]
1.32	11.6	720	23.4	68.9	MAPb$_{0.4}$Sn$_{0.6}$ Br$_{0.2}$I$_{2.8}$	[2]
1.33	7.5	450	24.9	67.0	CsSnI$_3$:MBAA	[2]
1.34	10.0	767	20.5	63.6	MAPb$_{0.4}$Sn$_{0.6}$I$_3$	[2]
1.34	12.1	780	20.7	75.1	MAPb$_{0.4}$Sn$_{0.6}$I$_{2.6}$Br$_{0.4}$	[2]
1.35	16.3	780	26.5	79.0	FAPb$_{0.7}$Sn$_{0.3}$I$_3$	[2]
1.36	8.2	630	19.7	66.1	CsSnI$_3$	[2]
1.37	14.7	737	27.1	73.6	FA$_{0.3}$MA$_{0.7}$Pb$_{0.7}$Sn$_{0.3}$I$_3$	[2]
1.38	17.3	810	28.2	75.4	FAPb$_{0.75}$Sn$_{0.25}$I$_3$	[2]
1.38	15.2	800	26.2	72.5	MAPb$_{0.75}$Sn$_{0.25}$I$_3$	[2]
1.39	20.6	1020	26.6	76.0	FA$_{0.7}$MA$_{0.3}$Pb$_{0.7}$Sn$_{0.3}$I$_3$	[2]
1.40	8.2	745	17.7	61.8	MAPb$_{0.6}$Sn$_{0.4}$I$_3$	[2]
1.40	**10.1**	**655**	**22.1**	**69.6**	**FASnI$_3$ + DipI + NaBH$_4$**	[49]

Table 3. Continued.

E_g [eV]	PCE [%]	V_{oc} [mV]	J_{sc} [mA cm^{-2}]	FF [%]	Absorber perovskite	Refs.
1.41	5.9	487	20.0	60.6	FA$_{1-x}$Rb$_x$SnI$_3$	[2]
1.42	**14.3**	**920**	**20.4**	**76.2**	**FASnI$_3$**	[51]
1.42	14.4	820	22.4	78.0	MAPb$_{0.75}$Sn$_{0.25}$I$_3$	[2]
1.42	13.2	840	20.3	78.0	EA$_{0.098}$EDA$_{0.01}$FA$_{0.882}$SnI$_3$	[2]
1.43	12.4	949	17.4	74.9	FA$_{0.85}$PEA$_{0.15}$SnI$_3$:NH$_4$SCN	[2]a)
1.44	**12.3**	**750**	**21.7**	**75.3**	**EA$_{0.098}$EDA$_{0.01}$FA$_{0.882}$SnI$_3$**	[52]
1.44	10.1	642	22.2	70.8	Cs$_{0.2}$FA$_{0.8}$SnI$_3$	[2]a)
1.44	10.2	638	22.0	72.5	FASnI$_3$:FOEI	[2]a)
1.45	**13.6**	**840**	**22.9**	**70.8**	**FASnI$_3$**	[53]
1.48	6.0	460	23.9	53.9	CsSnI$_3$	[2]
1.49	22.3	1090	26.3	78.0	FA$_{0.6}$MA$_{0.4}$PbI$_3$ (sc)	[2]
1.51	19.3	1047	23.8	77.5	FA$_{0.6}$MA$_{0.4}$PbI$_3$	[2]
1.52	22.0	1120	24.9	78.6	FA$_{0.85}$MA$_{0.15}$PbI$_3$	[2]
1.52	**25.3**	**1150**	**26.2**	**83.9**	**Cs$_{0.05}$FA$_{0.85}$MA$_{0.05}$Rb$_{0.05}$PbBr$_{0.15}$I$_{2.85}$**	[22]
1.52	24.1	1161	25.4	81.4	Cs$_{0.05}$FA$_{0.85}$MA$_{0.05}$Rb$_{0.05}$PbBr$_{0.15}$I$_{2.85}$	[22]a)
1.53	**24.0**	**1180**	**24.9**	**81.7**	**FA$_x$MA$_{1-x}$PbI$_3$**	[54]
1.53	**24.5**	**1158**	**25.3**	**83.8**	**FA$_{0.97}$MA$_{0.03}$PbI$_{2.91}$Br$_{0.09}$**	[55]
1.53	24.5	1185	26.1	79.1	α-FAPbI$_3$	[2]
1.53	25.2	1174	26.2	81.8	α-FAPbI$_3$	[2]a)
1.53	**25.4**	**1174**	**26.4**	**81.9**	**FAPbI$_3$**	[17]
1.53	25.5	1189	25.7	83.2	b)	[2]a)
1.54	24.6	1181	26.2	79.6	FAPbI$_3$	[2]a)
1.54	**25.6**	**1182**	**26.2**	**82.6**	**FAPbI$_3$: (PbI$_2$)$_2$RbCl**	[56]a)
1.54	**24.3**	**1141**	**25.7**	**82.6**	**Cs$_{0.03}$FA$_{0.97}$ Pb Br$_{0.09}$I$_{2.91}$**	[57]
1.54	25.7	1179	25.8	84.5	b)	[3]a)
1.55	**24.1**	**1158**	**25.3**	**82.3**	**FA$_{0.95}$MA$_{0.05}$PbBr$_{0.15}$I$_{2.85}$**	[58]
1.56	**25.1**	**1195**	**24.9**	**84.4**	**FA$_{0.995}$MA$_{0.005}$PbBr$_{0.015}$I$_{0.985}$**	[59]
1.56	25.2	1180	24.1	84.8	b)	[2]a)
1.56	25.2	1181	25.1	84.8	FAMAPb(IBrCl)$_3$	[2]a)
1.56	25.3	1193	25.1	84.6	FAMAPb(IBrCl)$_3$	[2]
1.57	23.0	1170	24.1	81.6	Cs$_{0.05}$FA$_{0.88}$MA$_{0.07}$PbBr$_{0.24}$I$_{2.76}$	[2]
1.57	**23.0**	**1147**	**25.1**	**79.9**	**FA$_{0.95}$MA$_{0.05}$PbBr$_{0.15}$I$_{2.85}$**	[60]a)
1.57	**23.4**	**1153**	**25.2**	**80.6**	**Cs$_{0.05}$FA$_{0.75}$MA$_{0.15}$Rb$_{0.05}$PbBr$_{0.15}$I$_{2.85}$**	[61]
1.58	**22.9**	**1173**	**23.4**	**80.0**	**Cs$_{0.05}$FA$_{0.9}$MA$_{0.05}$PbBr$_{0.26}$I$_{2.74}$**	[19]
1.58	22.6	1186	24.2	78.6	FA$_{0.92}$MA$_{0.08}$PbBr$_{0.24}$I$_{2.76}$	[2]a)
1.58	22.6	1178	22.73	84.4	b)	[2]a)
1.59	21.1	1086	24.0	81.0	MAPb$_{0.9}$Sn$_{0.05}$Cu$_{0.05}$I$_{2.9}$Br$_{0.1}$	[2]
1.59	21.0	1140	23.7	77.7	FA$_{0.85}$MA$_{0.15}$PbBr$_{0.45}$I$_{2.55}$	[2]a)
1.60	**21.9**	**1192**	**22.8**	**80.6**	**GA(MA)$_5$Pb$_5$I$_{16}$**	[62]
1.60	21.9	1131	23.1	83.7	CsMAFAPbI$_3$:PPP	[2]
1.60	20.3	1130	23.2	77.4	MAPbI$_{3-x}$Cl$_x$	[2]a)
1.61	21.4	1120	23.1	82.9	MAPbI$_3$	[2]c)
1.61	21.5	1192	21.6	83.6	Cs$_{0.05}$FA$_{0.88}$MA$_{0.07}$PbBr$_{0.44}$I$_{2.56}$	[2]a)

Table 3. Continued.

E_g [eV]	PCE [%]	V_{oc} [mV]	J_{sc} [mA cm^{-2}]	FF [%]	Absorber perovskite	Refs.
1.61	23.2	1240	22.1	84.5	$Cs_{0.05}FA_{0.88}MA_{0.07}PbBr_{0.44}I_{2.56}$	[2]
1.61	22.6	1200	24.0	78.5	$Cs_{0.07}FA_{0.765}MA_{0.135}Rb_{0.03}PbBr_{0.45}I_{2.55}$	[2]
1.62	21.7	1180	22.5	81.7	$MAPbI_3$-DAP	[2]
1.63	20.3	1130	23.4	76.8	$Cs_{0.05}FA_{0.76}MA_{0.19}PbBr_{0.6}I_{2.4}$	[2]
1.64	**22.4**	**1130**	**23.7**	**83.8**	**$Cs_{0.05}MA_{0.1425}FA_{0.8075}PbBr_{0.45}I_{2.55}$**	[63]
1.64	20.4	1140	23.6	75.8	$Cs_{0.05}FA_{0.79}MA_{0.16}PbBr_{0.51}I_{2.49}$	[2]
1.65	**21.9**	**1230**	**21.2**	**84.0**	**$Cs_{0.1}FA_{0.2}MA_{0.7}PbBr_{0.45}I_{0.55}$**	[64]
1.65	16.2	1109	19.6	74.2	$MAPbI_{1-x}Br_x$	[2][a]
1.66	10.4	904	16.3	70.4	$MAPbBr_{0.39}I_{2.51}$	[2]
1.67	17.9	1190	18.4	81.9	$(PEA)_2(MA)_3Pb_4I_{13}{:}NH_4I_{0.2}Cl_{0.8}$	[2]
1.68	20.7	1220	21.3	79.7	$Cs_{0.05}MA_{0.15}FA_{0.8}PbBr_{0.75}I_{2.25}$	[2]
1.69	7.1	936	10.4	63.0	$MAPbBr_{0.78}I_{2.22}$	[2]
1.70	**20.2**	**1176**	**20.8**	**82.5**	**$CsPbI_3$**	[65]
1.70	**20.1**	**1177**	**20.6**	**82.8**	**$CsPbI_3$**	[65][a),d)]
1.70	16.9	1170	20.2	71.5	$Cs_{0.2}FA_{0.8}PbBr_{0.75}I_{2.25}$	[2]
1.71	14.6	1056	17.5	79.0	$CsPbI_3$	[2]
1.72	18.6	1244	19.2	77.9	$Cs_{0.83}FA_{0.17}PbBr_{0.8}I_{2.2}$	[2]
1.72	18.3	1350	17.6	77.0	$MAPbBr_{0.6}I_{2.4}$	[2]
1.72	17.1	1200	19.4	73.5	$Cs_{0.17}FA_{0.83}PbBr_{1.2}I_{1.8}$	[2]
1.74	18.3	1269	18.9	76.3	$Cs_{0.095}MA_{0.1425}FA_{0.7125}Rb_{0.05}PbBrI_2$	[2]
1.74	**20.2**	**1210**	**19.3**	**86.5**	**$Cs_{0.2}FA_{0.8}PbBr_{0.9}I_{2.1}$**	[20]
1.75	19.8	1310	19.4	78.0	$Cs_{0.17}FA_{0.83}Pb(I_{0.6}Br_{0.4})_3$	[2]
1.76	18.5	1210	20.0	76.4	$Cs_{0.05}FA_{0.79}MA_{0.16}PbBr_{1.2}I_{1.8}$	[2]
1.77	18.6	1234	18.3	82.5	$CsPbI_{3-x}Br_x$	[2]
1.78	**17.3**	**1227**	**17.4**	**81.2**	**$Cs_{0.2}FA_{0.8}PbBr_{1.14}I_{1.86}$**	[36]
1.79	19.0	1250	19.0	80.0	$Cs_{0.12}MA_{0.05}FA_{0.83}PbBr_{1.2}I_{1.8}$	[2]
1.79	**17.7**	**1255**	**17.4**	**81.1**	**$Cs_{0.4}DMA_{0.1}FA_{0.5}PbBr_{0.71}Cl_{0.15}I_{2.14}$**	[66]
1.79	16.5	1284	17.2	74.8	$Cs_{0.17}FA_{0.83}PbBrI_{1.2}I_{1.8}$	[2]
1.80	13.7	1272	14.4	75.0	$MAPbBrI_2$	[2]
1.81	16.3	1220	17.0	78.6	$Cs_{0.4}FA_{0.6}PbBr_{1.05}I_{1.95}$	[2]
1.82	**17.2**	**1266**	**16.8**	**80.9**	**$Cs_{0.35}FA_{0.65}PbBr_{1.2}I_{1.8}$**	[67]
1.83	**16.9**	**1240**	**16.9**	**80.7**	**$FA_{0.6}MA_{0.4}PbBr_{1.2}I_{1.8}$**	[68]
1.84	15.2	1260	15.6	77.3	$Cs_{0.2}FA_{0.8}PbBr_{1.2}I_{1.8}$-DAP	[2]
1.85	15.0	1296	15.6	74.2	$Cs_{0.17}FA_{0.83}PbI_{1.5}Br_{1.5}$	[2]
1.86	17.0	1340	15.9	79.8	$CsPbBr_{0.75}I_{2.25}$-0.5FAOAc	[2]
1.87	14.0	1280	14.0	78.1	$CsBa_{0.2}Pb_{0.8}BrI_2$	[2]
1.87	13.7	1220	14.6	76.8	$CsEu_{0.05}Pb_{0.95}BrI_2$	[2]
1.88	**17.4**	**1420**	**15.0**	**81.4**	**$CsPbBrI_2$**	[69]
1.88	15.9	1300	15.5	79.1	$CsPbBrI_2$	[2]
1.88	15.3	1250	15.4	79.0	$CsPbBrI_2$	[2]
1.89	16.0	1310	15.8	77.5	$CsPbBrI_2$	[2]
1.89	15.6	1300	15.3	78.3	$CsPbBr(Ac)_xI_{2-x}$	[2]
1.90	15.0	1240	16.0	75.6	$InCl_3{:}CsPbI_2Br$	[2][a]

Table 3. Continued.

E_g [eV]	PCE [%]	V_{oc} [mV]	J_{sc} [mA cm^{-2}]	FF [%]	Absorber perovskite	Refs.
1.90	16.1	1320	15.3	79.7	$CsPbI_2Br$	[2]
1.91	14.4	1312	15.6	70.1	$FA_{0.17}Cs_{0.83}PbI_{1.2}Br_{1.8}$	[2]
1.91	14.2	1160	15.7	77.9	$CsPbI_2Br$	[2]
1.91	2.0	620	5.4	60.8	$MA_3Sb_2I_9$ + HI	[2]c)
1.94	**13.4**	**1240**	**14.2**	**76.0**	**$CsPbI_{1.8}Br_{1.2}$**	[70]
1.98	8.3	1080	12.3	62.0	$CsPbBr_2I$	[2]
2.00	9.6	1185	11.2	72.3	$Cs_{0.15}FA_{0.85}PbBr_{2.1}I_{0.9}$	[2]
2.03	2.8	836	6.4	52.7	$MAPbBr_{1.77}I_{1.23}$	[2]
2.04	10.3	1340	9.7	79.2	$MAPb(I_{0.3}Br_{0.7})_xCl_{3-x}$	[2]
2.05	6.1	1450	5.4	77.1	$MAPbBr_2I$	[2]
2.09	10.2	1270	11.5	69.4	$CsPbBr_2I$	[2]
2.10	10.7	1261	11.8	72.0	$CsPbBr_2I$	[2]
2.11	9.2	1200	10.2	74.6	GAI-DEE-$CsPbBr_2I$	[2]
2.14	3.1	650	8.1	58.4	$MASbSI_2$	[2]
2.15	4.4	1084	6.3	64.8	$FA_{0.85}MA_{0.15}PbBr_{0.45}I_{2.55}$; $R = 0.7$	[2]
2.19	2.0	1051	3.0	69.5	$FA_{0.85}MA_{0.15}PbBr_{0.45}I_{2.55}$; $R = 0.56$	[2]
2.20	**8.9**	**1639**	**7.7**	**70.6**	**$FAPbBr_3$**	[71]
2.27	10.6	1552	8.9	76.5	$FAPbBr_3$	[2]
2.28	10.5	1520	8.3	83.0	$CsPbBr_3$	[72]
2.29	**10.2**	**1650**	**8.7**	**71.1**	**$MAPbBr_3$**	[73]
2.31	9.7	1458	8.1	81.9	$CsPbBr_3$	[2]
2.32	10.1	1653	7.7	79.1	$MAPbBr_3$	[2]
2.33	8.5	1580	6.6	82.0	$CsPbBr_3$	[2]
2.33	8.2	1470	7.3	76.1	$CsPbBr_3$	[2]
2.34	**10.7**	**1635**	**7.8**	**84.1**	**$CsPbBr_3$**	[74]
2.34	10.1	1602	7.9	80.0	$CsPbBr_3$	[2]
2.34	9.7	1584	7.4	82.8	$CsPbBr_3$	[2]
2.35	10.7	1622	7.9	83.5	$CsPbBr_3$	[2]
2.35	10.6	1610	7.8	84.4	$CsSnBr_3$	[2]
2.35	**10.2**	**1611**	**7.8**	**81.0**	**$CsPbBr_3$**	[75]
2.36	10.3	1570	8.2	79.6	$CsPb_{0.97}Tb_{0.03}Br_3$	[76]
2.36	4.0	1130	5.5	63.6	$CsPbBr_{2.9}I_{0.1}$	[2]
2.37	2.2	690	5.0	63.5	$MA_3Sb_2Cl_xI_{9-x}$	[2]
2.38	8.1	1490	6.9	78.8	$CsPbBr_3$	[2]
2.41	2.7	1020	5.2	51.2	$Cs_2AgBiBr_6$	[2]
2.42	1.1	870	2.9	43.0	$BdAPbI_4$	[2]
2.43	2.8	820	5.7	60.3	$CsPb_2Br_5$	[2]
2.44	2.4	1140	3.4	60.9	$FAPbBr_{2.1}Cl_{0.9}$	[2]
2.45	2.9	1010	4.1	70.9	$Cs_2AgBiBr_6$	[2]
2.46	1.7	1060	3.9	40.2	$Cs_2AgBiBr_6$	[2]
2.47	**3.3**	**1278**	**3.3**	**77.5**	**$Cs_2AgBiBr_6$**	[77]
2.48	1.4	1060	2.5	52.0	$FAPbBr_2Cl$	[2]

a)Certified efficiency; b)Exception included as a material highlight; c)Exception included as a PCE highlight without the absorber information; d)PCE from J–V with significant hysteresis and MPP tracking closer to the listed value; sc, single crystal.

Table 4. Single junction organic research solar cells with the highest efficiency: performance parameters as a function of device absorber bandgap energy (from EQE spectrum).

Table 4. Continued.

E_g [eV]	PCE [%]	V_{oc} [mV]	J_{sc} [mA cm^{-2}]	FF [%]	Absorber blend	Refs.
1.22	13.4	663	30.0	67.1	BTB7-Th:ATT-9	[27]
1.32	13.0	916	20.2	70.1	BTR:Y6:bisPC$_{71}$BM	[78]
1.32	10.6	690	24.3	63.2	PTB7-Th:IEICO-4F	[2]
1.33	13.9	865	22.4	71.4	BTR:MeIC:Y11	[79]
1.34	12.8	712	27.3	65.9	PTB7-Th:IEICO-4F	[2]
1.35	17.0	804	27.2	76.4	PM6:mBzS-4F	[2]
1.35	15.9	820	26.3	73.4	PM6:Y6	[2]
1.36	15.9	846	25.4	74.1	PM6:Y11	[2]a)
1.37	18.3	856	26.9	79.4	PM6:BTP-eC9:PC$_{71}$BM	[2]
1.38	18.2	857	27.4	77.6	PM6:BTP-T-3Cl:BTP-4Cl-BO	[80]
1.38	18.8	861	27.5	79.4	PM6:BTP-eC9:BTP-S9	[81]
1.38	18.7	853	27.4	80.0	PM6:BTP-eC9:L8-BO-F	[82]
1.38	18.2	847	27.3	78.8	PM6:BTP-eC9:L8-BO-F	[82]a)
1.38	18.7	862	27.4	79.3	PM6:BTP-eC9:BTP-S9	[81]a)
1.39	18.1	848	27.5	77.5	PM6:Y6-1O:BO-4Cl	[83]a)
1.39	18.2	859	27.7	76.6	D18:Y6	[2]a)
1.39	18.5	855	27.5	78.9	PM6:Y6-1O:BO-4Cl	[83]
1.39	18.4	858	26.9	79.7	PB2:PBDB-TF:BTP-eC9	[84]
1.39	18.3	872	26.6	78.9	PM6:BTP-eC11:BTP-S2	[85]
1.39	18.2	863	27.1	77.9	PM6:BTP-eC9:ZY-4Cl	[86]a)
1.39	18.7	863	27.4	79.0	PM6:BTP-eC9:ZY-4Cl	[86]
1.40	19.1	869	27.5	79.9	PBDB-TF:L8-BO:BTP-eC9	[87]a)
1.40	19.4	863	27.6	81.2	PBDB-TF:L8-BO:BTP-eC9	[87]
1.40	18.1	867	26.8	78.0	PM6:AC9	[88]a)
1.40	18.1	868	26.4	78.8	PM6:CNS-6-8:Y6:PC$_{71}$BM	[89]
1.40	18.4	871	26.8	79.1	PM6:AC9	[88]
1.40	18.3	845	27.5	78.8	PTzBI-dF:BTP-TBr	[90]
1.41	17.6	871	26.4	76.8	D18-Cl:PM6:Y6	[2]
1.41	18.1	860	26.5	79.4	PM6:PB2F:BTP-eC9	[91]
1.41	19.0	879	26.7	81.0	PBQx-TF:eC9-2Cl:F-BTA3	[92]
1.41	18.7	878	26.8	79.4	PBQx-TF:eC9-2Cl:F-BTA3	[92]a)
1.42	15.6	834	24.9	75.1	PBDB-TF:BTP-4F	[2]
1.42	15.6	838	25.0	74.4	b)	[2]a)
1.43	18.2	880	25.9	80.1	PBDB-T-2F:BTP-4F-P2EH	[93]
1.43	14.3	820	24.9	70.0	PM6:IDST-4F	[2]
1.44	16.1	955	22.7	74.3	PM6:PY-IT:BN-T	[2]
1.44	18.6	893	26.0	80.0	PM6:L8-BO	[94]
1.44	18.2	883	26.1	79.0	PM6:L8-BO	[94]a)
1.45	19.6	896	26.7	81.9	PM6:D18:L8-BO	[25]
1.45	19.1	918	26.9	77.3	D18:L8-BO	[26]
1.45	19.2	891	26.7	80.7	PM6:D18:L8-BO	[25]a)
1.46	18.2	897	25.7	78.9	b)	[2]a)
1.46	16.8	949	23.7	74.4	PM6:PY-DT	[95]
1.47	14.6	882	23.1	71.7	PBDB-T-2Cl:BP-4F:MF1	[2]
1.48	12.4	880	20.8	67.7	PBDB-T:IDT-EDOT:PC$_{71}$BM	[2]
1.50	15.4	920	22.6	74.1	PM6:DTTC-4Cl	[2]
1.51	13.3	780	22.9	75.0	PM6:SeTlC4Cl-DIO	[2]
1.52	10.4	850	18.0	68.0	PBDB-T:IDT-EDOT:PC$_{71}$BM	[2]
1.53	10.7	850	22.2	56.7	PM6:SeTlC4Cl	[2]
1.54	13.6	940	19.5	73.8	BTR:NITI:PC$_{71}$BM	[2]
1.55	12.0	840	19.5	73.3	PM6:IT-4F	[2]
1.56	12.1	826	20.9	70.1	PBDB-T-2F:IT-4F	[2]
1.58	13.9	950	21.7	67.4	PM6:DTTC-4F	[2]
1.58	13.5	880	20.6	74.53	PBDB-T-SF:IT-4F	[2]
1.61	13.4	940	20.2	70.5	PM6:DTC-4F	[2]
1.61	12.1	916	18.1	73.0	PBDB-T-2Cl:MF1	[2]
1.62	11.0	793	19.4	71.5	b)	[2]a)
1.62	12.2	930	17.5	75.0	PTQ10:IDTPC	[2]
1.63	12.8	910	19.1	73.6	PTQ10:IDIC-2F	[2]
1.64	12.9	960	17.4	71.3	PTQ10:IDIC	[2]
1.65	9.3	820	16.5	68.7	J51:ITIC	[2]
1.66	12.1	815	20.3	73.2	b)	[2]a)
1.67	10.2	810	21.0	59.9	P4TIF:PC$_{61}$BM	[2]
1.67	11.5	791	19.7	73.7	b)	[2]a)
1.68	12.0	1030	18.5	63.0	PBDTTT-EFT:EHIDTBR	[2]
1.69	8.9	878	13.9	72.9	PBT1-C:NFA	[2]
1.70	11.1	867	17.8	71.9	b)	[2]a)
1.72	10.0	899	16.8	66.4	b)	[2]a)
1.76	9.6	786	17.0	72.0	PPDT2FBT:PC$_{70}$BM	[2]
1.79	7.5	1140	10.6	62.1	BDT-ffBX-DT:PDI4	[2]
1.79	6.2	1230	8.9	56.6	BDT-ffBX-DT:SFPDI	[2]
1.85	9.0	900	13.8	72.9	BTR:PC$_{71}$BM	[2]
1.85	7.6	830	13.3	69.1	PBDB-T:PC$_{71}$BM	[2]
1.86	7.4	940	12.7	61.9	PBDB-T:NDP-Se-DIO	[2]
1.88	5.7	950	10.7	55.9	PBDB-T-2Cl:PC61BM	[2]
1.93	6.3	790	12.2	65.3	P3HT:TCBD14	[2]
2.01	3.7	592	10.4	59.2	P3HT:PCBM	[2]

a)Certified efficiency; b)Exception included as a PCE highlight without the absorber information.

Table 5. Single junction dye sensitized research solar cells with the highest efficiency: performance parameters as a function of device absorber bandgap energy (from EQE spectrum).

E_g [eV]	PCE [%]	V_{oc} [mV]	J_{sc} [mA cm^{-2}]	FF [%]	Sensitizing dye	Refs.
1.44	11.0	714	21.9	70.3	[b]	[2][a]
1.52	11.4	743	21.3	71.9	[b]	[2][a]
1.59	10.1	710	18.5	76.9	TF-tBu_C$_3$F$_7$	[2]
1.66	13.0	910	18.1	78.0	SM315	[96]
1.66	10.7	849	16.6	75.9	bJS2	[2]
1.74	7.8	694	15.4	72.7	YD2	[2]
1.75	10.9	745	20.7	70.8	YKP-88/YKP-137 (6/4)	[2]
1.76	12.0	960	15.9	79.0	SM371	[96]
1.77	10	740	18.1	74.7	N719	[2]
1.79	**9.9**	**740**	**19.0**	**70.5**	**PI-COF:N719**	[97]
1.80	9.1	744	19.0	64.0	N719	[2]
1.80	9.0	790	19.8	57.2	N719	[2]
1.80	6.5	663	13.3	74.5	SK7	[2]
1.81	**8.5**	**700**	**19.4**	**62.6**	**N719**	[98]
1.82	6.4	680	13.1	71.8	AN-11	[2]
1.83	**15.2**	**1063**	**18.0**	**79.4**	**SL9 + SL10/BPHA**	[14][a]
1.83	8.9	820	19.0	57.5	N719	[2]
1.85	12.3	1020	15.2	79.1	[b]	[2][a]
1.86	8.3	782	14.8	71.7	N719	[2]
1.87	9.1	1060	11.2	76.7	L351	[2]
1.88	7.8	730	14.3	74.7	TY4	[2]
1.93	11.2	1140	13.0	75.6	L350	[2]
1.97	3.0	600	6.3	79.4	AN-14	[2]
1.99	5.4	689	11.3	69.5	SK6	[2]
2.00	6.3	732	12.0	71.7	CW10 + SK6	[2]
2.01	9.2	1160	11	72.1	L349	[2]
2.02	8.1	760	14.3	75.0	TY6	[2]
2.05	3.9	680	7.4	77.5	AN-12	[2]
2.09	6.9	780	11.6	76.3	TY3	[2]
2.12	5.8	739	10.8	72.7	CW10	[2]
2.15	**4.1**	**640**	**8.76**	**73.6**	**PS1**	[99]
2.23	5.8	760	10.2	74.8	MS3	[2]
2.32	5.3	1170	6.4	70.8	L348	[2]

[a] Certified efficiency; [b] Exception included as a PCE highlight without the absorber information.

Table 6. Single junction research solar cells with the highest efficiency: performance parameters as a function of device absorber bandgap energy (from EQE spectrum) among several inorganic emerging technologies.

E_g [eV]	PCE [%]	V_{oc} [mV]	J_{sc} [mA cm^{-2}]	FF [%]	Absorber material/technology	Refs.
0.98	11.2	430	39.2	66.8	Cu$_2$ZnSn(Se,S)$_4$	[2]
1.02	11.6	441	39.2	67.4	Cu$_2$ZnSnSe$_4$	[2]
1.03	11.6	423	40.6	67.3	Cu$_2$ZnSnSe$_4$	[2][a]
1.04	9.6	425	34.9	64.5	Cu$_2$ZnSnSe$_4$	[2]
1.05	9.4	457	32.5	63.3	Cu$_2$ZnSnSe$_4$	[2]
1.06	9.5	460	31.1	66.4	Cu$_2$ZnSnSe$_4$	[2]
1.06	13.2	477	40.1	69.0	Cu$_2$ZnSn(S,Se)$_4$	[2]
1.06	12.7	461	40.4	68.3	Cu$_2$ZnSn(S,Se)$_4$	[2][a]
1.07	12.5	491	37.4	68.2	Cu$_2$ZnSnSe$_4$	[2][a]
1.08	12.4	522	33.3	71.3	Cu$_2$ZnSn(S,Se)$_4$	[2]
1.09	12.2	475	37.2	68.8	Cu$_2$ZnSn(S,Se)$_4$	[2]
1.09	12.5	540	32.1	72.1	(Ag,Cu)$_2$ZnSn(S,Se)$_4$	[2]
1.10	**13.6**	**538**	**36.2**	**69.9**	**Cu$_2$ZnSn(S,Se)$_4$**	[3]
1.11	**13.1**	**547**	**34.3**	**70.0**	**Cu$_2$ZnSn(S,Se)$_4$**	[28]
1.11	**12.8**	**526**	**35.3**	**68.9**	**Cu$_2$ZnSn(S,Se)$_4$**	[28][a]
1.12	12.3	527	32.3	72.3	Cu$_2$Zn(Sn$_{0.78}$Ge$_{0.22}$)Se$_4$	[2]
1.13	12.6	513	35.2	69.8	Cu$_2$ZnSn(S,Se)$_4$	[2][a]
1.13	11.1	460	34.5	69.8	Cu$_2$ZnSn(S,Se)$_4$	[2][a]
1.14	12.6	541	35.4	65.9	Cu$_2$ZnSn(S,Se)$_4$	[2][a]
1.16	11.2	539	33.1	62.8	Cu$_2$ZnSn(S,Se)$_4$	[2]
1.22	7.5	413	28.9	62.4	Sb$_2$Se$_3$	[2]
1.24	9.2	400	32.6	70.6	Sb$_2$Se$_3$	[2]
1.27	4.8	370	27.3	47.3	Sb$_2$Se$_3$	[2]
1.29	4.0	340	22.9	51.0	Sb$_2$Se$_3$	[2]
1.31	7.3	420	29.2	59.7	Sb$_2$Se$_3$	[2]
1.33	**8.6**	**520**	**27.8**	**59.8**	**Sb$_2$Se$_3$**	[100]
1.37	**7.1**	**480**	**24.7**	**60.0**	**AgBiS$_2$**	[101]
1.39	**8.9**	**482**	**26.8**	**68.5**	**AgBiS$_2$**	[32][a]
1.39	**9.2**	**495**	**27.1**	**68.4**	**AgBiS$_2$**	[32]
1.45	8.5	625	24.4	55.7	Cu$_2$ZnGeSe$_4$	[2]
1.50	11.0	731	21.7	69.3	Cu$_2$ZnSnS$_4$	[2][a]
1.50	10.0	655	24.1	63.3	Sb$_2$(S,Se)$_3$	[31][a]
1.52	8.7	664	20.6	63.9	(Cu$_{0.99}$Ag$_{0.01}$)$_{1.85}$(Zn$_{0.8}$Cd$_{0.2}$)$_{1.1}$SnS$_4$	[2]
1.53	4.1	473	14.8	58.7	SbSeI:Sb$_2$Se$_3$	[2]
1.54	**10.7**	**673**	**23.7**	**66.8**	**Sb$_2$(S,Se)$_3$**	[15]
1.54	9.7	638	23.2	65.5	Sb$_2$(S,Se)$_3$	[102]
1.55	10.5	664	23.8	66.3	Sb$_2$(S,Se)$_3$	[30]
1.73	**8.0**	**757**	**60.5**	**17.4**	**Sb$_2$S$_3$**	[103]
1.80	7.5	711	16.1	65.0	Sb$_2$S$_3$	[2]

[a] Certified efficiency.

ADVANCED
SCIENCE NEWS

www.advancedsciencenews.com

ADVANCED
ENERGY
MATERIALS

www.advenergymat.de

Table 7. Single junction research solar cells with the highest efficiency: performance parameters as a function of device absorber bandgap energy (from EQE spectrum) among established technologies.

E_g [eV]	PCE [%]	V_{oc} [mV]	J_{sc} [mA cm^{-2}]	FF [%]	Absorber material/technology	Refs.
1.09	19.8	716	34.9	79.2	CIGS	[2][a]
1.10	21.7	718	40.7	74.3	CIGS	[2][a]
1.11	26.7	738	42.7	84.9	Si	[2][a]
1.13	22.9	744	38.8	79.5	CIGS	[2][a]
1.14	21.0	757	35.7	77.6	CIGS	[2][a]
1.15	23.4	734	39.6	80.4	CIGS	[2][a]
1.18	**20.0**	**706**	**40.7**	**69.7**	**Si**	[16]
1.30	16.3	762	31.4	68.1	CIGS	[2]
1.42	29.1	1127	29.8	86.7	GaAs	[2][a]
1.42	21.0	876	30.3	79.4	CdTe	[2][a]
1.48	18.3	857	27.0	77.0	CdTe	[2][a]
1.60	15.2	902	23.1	73	CIGS	[2]
1.60	10.2	896	16.4	69.8	Si (amorphous)	[2][a]
1.69	10.6	896	16.1	75.6	Si (amorphous)	[2]
1.85	10.1	886	16.8	67.0	Si (amorphous)	[2][a]

[a] Certified efficiency

Table 8. Monolithic multijunction perovskite-based research solar cells with the highest efficiency: performance parameters as a function of the device bandgap energies (from EQE spectra) of the subcells.

$E_{g,bottom}$ [eV]	$E_{g,middle}$, $E_{g,top}$ [eV]	PCE [%]	V_{oc} [mV]	J_{sc} [mA cm^{-2}]	FF [%]	Bottom absorber material	Middle, top absorber material(s)	Refs.
							Si/perovskite	
1.11	1.63	24.1	1786	19.5	69.1	Si	$Cs_xFA_{1-x}Pb(I,Br)_3$	[2]
1.11	1.66	26.0	1820	19.2	75.4	Si	$Cs_{0.1}MA_{0.9}PbBr_{0.3}I_{2.7}$	[2]
1.11	1.67	26.7	1756	19.2	79.2	Si	$PEA(I_{0.25}SCN_{0.75})$	[2]
1.11	1.68	25.7	1781	19.1	75.4	Si	$Cs_{0.05}FA_{0.8}MA_{0.15}PbBr_{0.75}I_{2.25}$	[2][a]
1.11	**1.69**	**29.8**	**1190**	**19.5**	**79.8**	**Si**	[b]	[3][a]
1.12	1.64	26.0	1760	19.2	76.5	Si	$FA_{0.83}MA_{0.17}PbI_3$	[2]
1.12	1.65	26.5	1760	19.4	77.0	Si	$Cs_{0.05}FA_{0.79}MA_{0.16}PbBr_{0.51}I_{2.49}$	[2]
1.12	1.68	28.8 (29.2)[c]	1895	19.2	78.9	Si	$Cs_{0.05}FA_{0.73}MA_{0.22}PbBr_{0.69}I_{2.31}$	[2]
1.13	**1.67**	**28.3**	**1776**	**20.1**	**79.6**	**Si**	**$FAMAPb(BrClI)_3$**	[37][a]
1.13	1.65	24.9	1735	19.5	73.5	Si	$CsFAPb(BrI)_3$	[2]
1.13	1.67	27.1	1886	19.1	75.3	Si	$CsFAMAPb(BrClI)_3$	[2]
1.13	1.69	29.5	1884	20.3	77.3	Si	[b]	[2]
1.14	**1.68**	**27.5**	**1779**	**19.6**	**78.9**	**Si**	**$Cs_{0.22}FA_{0.78}PbBr_{0.45}Cl_{0.09}I_{2.55}$**	[104]
1.14	**1.69**	**26.8**	**1891**	**17.8**	**79.4**	**Si**	[b]	[3][a]
1.14	**1.69**	**26.0**	**1780**	**18.2**	**80.2**	**Si**	**$Cs_{0.15}FA_{0.7055}MA_{0.1445}PbBr_{0.6}I_{2.4}$**	[105]
1.15	1.62	20.9	1690	15.9	77.6	Si	$MAPbI_3$	[2]
1.15	1.68	25.4	1800	17.8	79.4	Si	$Cs_{0.15}FA_{0.71}MA_{0.14}PbBr_{0.6}I_{2.4}$	[2]
1.15	1.68	25.0	1770	18.4	77.0	Si	$Cs_{0.25}FA_{0.75}PbBr_{0.6}I_{2.4}$	[2]
1.16	1.62	19.2	1701	16.1	70.1	Si	$MAPbI_3$	[2]

Table 8. Continued.

$E_{g,bottom}$ [eV]	$E_{g,middle}$, $E_{g,top}$ [eV]	PCE [%]	V_{oc} [mV]	J_{sc} [mA cm^{-2}]	FF [%]	Bottom absorber material	Middle, top absorber material(s)	Refs.
						GaAs/perovskite		
1.42	1.85	24.3	2160	14.3	78.8	GaAs	$Cs_{0.16}FA_{0.80}MA_{0.04}PbBr_{1.50}I_{1.50}$	[2]
						CIGS/perovskite		
1.01	**1.61**	**24.3**	**1570**	**21.0**	**73.6**	**CuInSe$_2$**	**$Cs_{0.05}FA_{0.85}MA_{0.1}PbI_{2.7}Br_{0.3}$**	[35]
1.01	**1.61**	**23.5**	**1590**	**19.4**	**75.5**	**CuInSe$_2$**	**$Cs_{0.05}FA_{0.85}MA_{0.1}PbI_{2.7}Br_{0.3}$**	[35][a]
1.10	1.65	22.4	1774	17.3	73.1	CIGS	$Cs_{0.09}FA_{0.77}MA_{0.14}PbBr_{0.42}I_{2.58}$	[2][b]
1.11	1.64	21.6	1580	18.0	76.0	CIGS	$Cs_{0.05}FA_{0.7885}MA_{0.1615}PbBr_{0.51}I_{2.49}$	[2]
1.11	1.65	23.3	1680	19.2	71.9	CIGS	$Cs_{0.05}FA_{0.7885}MA_{0.1615}PbBr_{0.51}I_{2.49}$	[2]
1.11	**1.68**	**24.2**	**1770**	**18.8**	**71.2**	**CIGS**	**$Cs_{0.05}FA_{0.7315}MA_{0.2185}PbBr_{0.69}I_{2.31}$**	[106]
1.12	1.68	24.2	1768	19.2	72.9	CIGS	[b]	[2][a]
						Perovskite/perovskite		
1.25	**1.80**	**26.3 (26.4)[c]**	**2044**	**16.5**	**78.1**	**$Cs_{0.2}FA_{0.8}Pb Br_{1.14}I_{1.86}$**	**$FA_{0.7}MA_{0.3}Pb_{0.5}Sn_{0.5}I_3$**	[36][a],[d]
1.26	**1.79**	**23.1**	**1950**	**15.8**	**75.0**	**$FA_{0.66}MA_{0.34}Pb_{0.5}Sn_{0.5}I_3$**	**$Cs_{0.05}(FAMA_{0.95})K_{0.05}Pb(BrI)_3$**	[107]
1.26	1.80	28.0	2125	16.42	80.2	[b]	[b]	[3][a]
1.26	**1.80**	**26.2**	**2040**	**16**	**80.1**	**$FA_{0.7}MA_{0.3}Pb_{0.5}Sn_{0.5}I_3$**	**$Cs_{0.4}DMA_{0.1}FA_{0.5}PbBr_{0.71}Cl_{0.15}I_{2.14}$**	[66]
1.26	1.82	24.0	1986	15.8	76.6	$FSA:FA_{0.7}MA_{0.3}Pb_{0.5}Sn_{0.5}I_3$	$Cs_{0.2}FA_{0.8}PbBr_{1.2}I_{1.8}$	[2][a]
1.26	1.82	25.5	2009	15.9	79.8	$FSA:FA_{0.7}MA_{0.3}Pb_{0.5}Sn_{0.5}I_3$	$Cs_{0.2}FA_{0.8}PbBr_{1.2}I_{1.8}$	[2]
1.27	1.72	22.9	1915	15.0	79.8	$FA_{0.6}MA_{0.4}Pb_{0.4}Sn_{0.6}I_3$	$Cs_{0.05}FA_{0.8}MA_{0.15}Pb Br_{0.45}I_{2.55}$	[2]
1.27	1.81	24.3	2030	15.2	78.8	$Cs_{0.05}FA_{0.5}MA_{0.45}Pb_{0.5}Sn_{0.5}I_3$	$Cs_{0.4}FA_{0.6}PbBr_{1.05}I_{1.95}$	[2]
1.27	1.81	24.5	1927	15.9	80.0	$FA_{0.7}MA_{0.3}Pb_{0.5}Sn_{0.5}I_3$	$Cs_{0.2}FA_{0.8}PbBr_{1.2}I_{1.8}$	[2]a
1.27	**1.82**	**23.2**	**1890**	**15.4**	**79.8**	**$Cs_{0.2}FA_{0.8}Pb_{0.5}Sn_{0.5}I_3$**	**$Cs_{0.2}FA_{0.8}PbBr_{1.2}I_{1.8}$**	[108]
1.28	1.73	23.1	1880	16.0	77.0	$Cs_{0.25}FA_{0.75}Pb_{0.5}Sn_{0.5}I_3$	$Cs_{0.3}DMA_{0.1}FA_{0.6}PbBr_{0.6}I_{2.4}$	[2]
						OPV/perovskite		
1.21	**1.83**	**21.7**	**1880**	**15.7**	**73.5**	**PTB7-Th:BTPV-4Cl-eC9**	**$FA_{0.6}MA_{0.4}PbBr_{1.2}I_{1.8}$**	[68]
1.25	1.91	15.0	1710	12.0	73.4	PTB7-Th:COi8DFIC:PC$_{71}$BM	$CsPbBrI_2$	[2]
1.38	1.91	21.1	1960	13.3	80.9	PM6:Y6-BO	$CsPbBrI_2$	[2]
1.38	**1.88**	**23.4**	**2136**	**14.6**	**75.2**	[b]	[b]	[3][a]
1.40	1.83	15.1	1850	11.5	71.0	PBDB-T:SN6IC-4F	$Cs_{0.1}FA_{0.54}MA_{0.36}PbBr_{1.4}I_{1.8}$	[2]
1.40	1.82	19.5	1925	13.1	77.2	PBDBT-2F:Y6:PC$_{71}$BM	$Cs_{0.18}FA_{0.8}MA_{0.02}PbBr_{1.2}I_{1.8}$	[2][a]
1.40	1.82	20.4	1902	13.1	81.5	PBDBT-2F:Y6:PC$_{71}$BM	$Cs_{0.18}FA_{0.8}MA_{0.02}PbBr_{1.2}I_{1.8}$	[2]
						DSSC/perovskite		
1.59	1.93	10.5	1170	12.9	70.0	$FA_{0.85}MA_{0.15}PbBr_{0.45}I_{2.49}$	N719	[2]
						Triple-junction		
1.13	**1.54, 1.91**	**20.1**	**2740**	**8.5**	**86.0**	**Si**	**$Cs_{0.1}FA_{0.9}PbI_3$, $Cs_{0.2}FA_{0.8}PbBr_{1.65}I_{1.35}$**	[38]
1.23	1.57, 1.78	16.8	2780	7.4	81	$FA_{0.66}MA_{0.34}Pb_{0.5}Sn_{0.5}I_3$	$FA_{0.66}MA_{0.34}Pb Br_{0.15}I_{2.85}$, $Cs_{0.1}FA_{0.594}MA_{0.306}PbBrI_2$	[109]
1.26	1.65, 2.06	19.9	2793	8.8	80.7	$FA_{0.7}MA_{0.3}Pb_{0.5}Sn_{0.5}I_3$	$Cs_{0.05}FA_{0.95}PbBr_{0.45}I_{2.55}$, $Cs_{0.2}FA_{0.8}PbBr_{2.1}I_{0.9}$	[39]

[a]Certified efficiency; [b]Exception included as a PCE highlight without the absorber material information; [c]In the parenthesis the certified efficiency from MPP tracking.

ADVANCED
SCIENCE NEWS
www.advancedsciencenews.com

ADVANCED
ENERGY
MATERIALS
www.advenergymat.de

Table 9. Monolithic multijunction organic- and dye sensitized-based research solar cells with the highest efficiency: performance parameters as a function of the device bandgap energies (from EQE spectra) of the subcells.

$E_{g,bottom}$ [eV]	$E_{g,top}$ [eV]	PCE [%]	V_{oc} [mV]	J_{sc} [mA cm^{-2}]	FF [%]	Bottom absorber	Top absorber	Refs.
						OPV/OPV		
1.23	1.66	16.4	1650	14.5	68.5	PTB7-Th:BTPV-4F:PC$_{71}$BM	PM6:m-DTC-2F	[2]
1.24	1.72	17.3	1640	14.4	73.3	PTB7-Th:O6T-4F:PC$_{71}$BM	PBDB-T:F-M	[2]
1.31	1.64	15.9	1660	14.1	68.0	PM6:SFT8-4F	PCE-10:BT-CIC:BEIT-4F	[2]
1.32	1.65	15.0	1600	13.6	69.0	PTB7-Th:PCDTBT:IEICO-4F	PBDB-T-2F:TfIF-4FIC	[2]
1.32	1.74	19.6	1910	14.2	72.4	PBDB-TF:ITCC	PBDB-TF:BTP-eC11	[2]
1.32	1.74	19.5	1912	14.2	72.0	PBDB-TF:ITCC	PBDB-TF:BTP-eC11	[2]
1.36	**1.73**	**18.7**	**1883**	**14.0**	**70.9**	**PM6:CH1007:PC$_{71}$BM**	**D18:F-ThBr**	[110]
1.37	1.73	15.2	1610	12.9	73.0	PM6:Y6	PV2000:PCBM	[2]
1.38	**1.80**	**20.3**	**2010**	**13.1**	**76.8**	**PBDB-TF:GS-ISO**	**PBDM-TF:BTp-eC9**	[111]
1.38	**1.80**	**20.3**	**2010**	**13.1**	**76.8**	**PBDB-TF:GS-ISO**	**PBDM-TF:BTp-eC9**	[111]
1.42	1.79	15.0	1590	13.3	71.0	PCE-10:BTCIC	DTDCPB:C$_{70}$	[2]
1.48	1.74	14.1	1710	11.7	70.0	PTB7-Th:NOBDT	PBDB-T: F-M	[2]
						OPV/a-Si		
1.33	1.78	15.1	1610	13.2	71.0	PTB7-Th:IEICO-4F	a-Si	[2]
						Si/DSSC		
1.11	1.84	14.7	580	40.9	62.0	Si	N719	[2]
1.24	1.67	17.2	1360	18.1	69.3	Si	SGT-021	[2]
						CIGS/DSSC		
1.21	1.82	13.0	1170	14.6	77.0	CIGS	N719	[2]
1.22	1.90	12.4	1435	14.1	61.0	CIGS	N719	[2]
1.22	1.82	15.1	1450	14.1	74.0	CIGS	N719	[2]
						DSSC/DSSC		
1.40	1.98	11.4	1400	12.2	66.7	DX1	N719	[2]
1.44	1.95	10.4	1450	10.8	67	N719	Black dye	[2]
1.67	1.98	12.3	1825	10.3	65	SGT-121/HC-A1	SGT-021/HC-A4	[112]
1.78	2.37	7.1	1420	7.2	69	N719	D131	[2]

Table 10. Monolithic multijunction research solar cells with the highest efficiency: performance parameters as a function of the device bandgap energies (from EQE spectra) of the subcells among other established technologies.

$E_{g,bottom}$ [eV]	$E_{g,middle}$, $E_{g,top}$, [eV]	PCE [%]	V_{oc} [mV]	J_{sc} [mA cm^{-2}]	FF [%]	Bottom absorber	Middle, top absorber(s)	Refs.
						GaAs/GaInP		
1.35	1.90	32.9	2500	15.4	85.7	GaAs	GaInP	[2]
1.41	1.88	32.8	2568	14.66	87.7	GaAs	GaInP	[2]
1.41	1.92	27.4	2400	13.1	88.0	GaAs	GaInP	[2]
1.42	1.85	31.6	2538	14.2	87.7	GaAs	GaInP	[2]
						Si/GaAsP		
1.17	1.90	23.4	1732	17.34	77.7	Si	GaAsP	[2]
						nc-Si/a-Si		
1.36	1.93	11.8	1428	12.27	67.5	nc-Si	a-Si	[2]
						Triple-junction cells		
0.92	**1.33, 1.88**	**39.5**	**3000**	**15.4**	**85.3**	**InGaAs**	**GaAs, InGaP**	[40]
0.98	1.41, 1.89	37.7	3014	14.6	86.0	InGaAs	GaAs, InGaP	[113]
1.13	1.48, 1.93	35.9	3248	13.1	84.3	Si	GaInAsP, InGaP	[114]
1.01	1.50, 1.92	28.1	2952	11.7	81.1	CIGS	AlGaAs/GaInP	[114]
1.30	1.27, 2.03	14.0	1922	9.9	73.4	nc-Si	nc-Si, a-Si	[115]

7.2. Best Performing Flexible Research Solar Cells Tables

All the experimental data are summarized in **Tables 11–16**.

Table 11. Flexible perovskite single junction research solar cells with the highest efficiency: performance parameters as a function of photovoltaic bandgap energy (from EQE spectrum).

E_g [eV]	PCE [%]	V_{oc} [mV]	J_{sc} [mA cm^{-2}]	FF [%]	Absorber perovskite	Refs.
1.41[b]	5.2	462	17.8	63.7	**FA$_{0.8}$MA$_{0.2}$SnBr$_{0.2}$I$_{2.8}$**	[116]
1.44	8.5	650	20.8	62.9	**FAGe$_{0.1}$Sn$_{0.9}$I$_3$**	[117]
1.47[b]	3.6	616	14.5	40.6	(5-AVA)$_\gamma$(MA)$_{1-\gamma}$PbI$_3$	[2]
1.53	20.5	1070	23.6	81.2	**FAMAPbI$_3$**	[117]
1.53	20.2	1123	24.7	72.9	FA$_{0.87}$MA$_{0.13}$PbCl$_x$I$_{3-x}$	[2]
1.54	22.4	1151	23.4	82.9	**FAMAPbI$_3$**	[118]
1.54	22.4	1170	24.6	77.8	**Cs$_{0.1}$FA$_{0.9}$PbI$_3$**	[119]
1.56	21.7	1127	24.8	77.7	**Cs$_{0.05}$FA$_{0.931}$MA$_{0.019}$PbBr$_{0.06}$I$_{2.94}$/ PM6:CH1007:PCBM**	[120]
1.56	20.8	1190	21.9	79.6	FA$_{0.95}$MA$_{0.05}$PbBr$_{0.15}$I$_{2.85}$	[2]
1.56	20.3	1160	23.4	74.8	FA$_{0.95}$MA$_{0.05}$PbBr$_{0.15}$I$_{2.85}$	[2]
1.56	19.9	1109	23.2	77.3	Cs$_{0.05}$FA$_{0.747}$MA$_{0.153}$Rb$_{0.05}$PbBr$_{0.15}$I$_{2.85}$	[2][a]
1.56	19.9	1192	21.9	76.3	FA$_{0.95}$MA$_{0.05}$PbBr$_{0.15}$I$_{2.85}$	[2][a]
1.57	19.5	1110	23.1	76.0	Cs$_{0.03}$FA$_{0.945}$MA$_{0.025}$PbBr$_{0.075}$I$_{2.925}$	[2]
1.58	19.2	1120	21.7	78.9	Cs$_{0.08}$FA$_{0.87}$MA$_{0.05}$PbBr$_{0.12}$I$_{2.88}$	[2]
1.59	19.9	1120	23.0	77.5	FAMAPb(BrI)$_3$	[2]
1.59	19.3	1090	22.7	78.1	MAPbI$_3$–NH4Cl	[2]
1.59	20.2	1120	22.2	81.1	**FAMAPbBrI**	[121]
1.60	20.6	1110	23.0	80.7	**CsFAMAPbBrI**	[122]
1.60	20.5	1140	23.5	76.5	**Cs$_{0.04}$FA$_{0.86}$MA$_{0.1}$PbBr$_{0.29}$I$_{2.71}$**	[123]
1.60	17.8	1060	21.8	77.3	**CsFAMAPbBrI**	[122][c]
1.61	17.3	1062	21.7	74.9	Cs$_{0.05}$FA$_{0.81}$MA$_{0.14}$PbBr$_{0.45}$I$_{2.55}$	[2][a]
1.61	19.1	1135	21.2	79.2	Cs$_{0.05}$FA$_{0.75}$K$_{0.04}$MA$_{0.15}$Rb$_{0.01}$PbBr$_{0.51}$I$_{2.49}$	[2]
1.62	20.1	1150	22.4	78.0	Cs$_{0.04}$FA$_{0.8064}$MA$_{0.1536}$PbBr$_{0.48}$I$_{2.52}$	[2]
1.62	18.0	1120	22.3	72.1	Cs$_{0.06}$FA$_{0.79}$MA$_{0.15}$PbBr$_{0.45}$I$_{2.55}$	[2]
1.63	14.9	1030	21.5	67.3	**MAPbI$_3$**	[124]
1.63	10.4	1030	19.2	52.8	FA$_{0.85}$MA$_{0.15}$PbBr$_{0.45}$I$_{2.55}$	[2]
1.65	11.2	940	18.4	64.9	MAPbI$_3$	[2]
1.65	7.9	1090	10.8	70.7	(α-FAPbI$_3$)$_{0.5}$(MAPbI$_2$Br)$_{0.5}$	[2]

[a]Certified efficiency; [b]E_g taken from absorption or photoluminescence spectra; [c]Exception included as a large-area highlight.

Table 12. Flexible organic single junction research solar cells with the highest efficiency: performance parameters as a function of photovoltaic bandgap energy (from EQE spectrum).

E_g [eV]	PCE [%]	V_{oc} [mV]	J_{sc} [mA cm^{-2}]	FF [%]	Absorber blend	Refs.
1.27	7.4	708	15.9	65.2	PTB7-Th:COi 8DFIC:PC$_{71}$BM	[2]
1.32	10.6	690	24.3	63.2	PTB7-Th:IEICO-4F	[2]
1.36	16.6	821	26.8	75.4	**PM6:BTP-4Cl-12**	[125]
1.37	16.1	840	25.0	76.7	PM6:N3:PC$_{71}$BM	[2]
1.38	12.0	827	21.6	67.4	**PM6:BTP-4Cl-12**	[125][a]
1.38	17.5	835	27.4	76.7	**PM6:BTP-eC9:PC$_{71}$BM**	[42]
1.39	16.1	820	25.9	75.8	PBDB-T-2F:BTP-eC9:PC$_{71}$BM	[2]
1.39	15.9	864	25.0	73.5	**D-18-Cl:G19:Y6**	[126]
1.40	16.1	860	25.9	74.7	PM6:Y6	[2]
1.40	15.2	832	25.1	73.0	PBDB-T-2F:Y6	[2]
1.40	17.1	830	27.4	74.9	**PBDB-T-2F:BTP-eC9:PC$_{71}$BM**	[127]
1.41	15.2	830	25.0	73.3	**PM6:Y6**	[128]
1.41	15.1	847	24.9	71.6	PM6:Y6:C6	[2]
1.42	16.6	860	25.9	74.7	PM6:Y6	[2]
1.44	10.4	848	17.0	72.2	PM6:Y6	[2]
1.55	12.0	840	19.5	73.3	PM6:IT-4F	[2]
1.56	11.6	820	19.6	72.2	PBDB-T-2F:IT-4F	[2]
1.56	12.1	826	20.9	70.1	PBDB-T-2F:IT-4F	[2]
1.61	10.9	900	18.7	64.8	PBDB-T:ITIC	[2]
1.63	9.2	770	16.0	74.7	PTB7-Th:PC$_{71}$BM	[2]
1.65	9.3	820	16.5	68.7	J51:ITIC	[2]
1.65	8.2	890	13.4	68.6	PBDB-T:ITIC	[2]
1.82	7.2	925	10.9	71.3	JP02	[2]
2.01	3.7	592	10.4	59.2	P3HT:PCBM	[2]

[a]Certified efficiency.

Table 13. Flexible dye sensitized single junction research solar cells with the highest efficiency: performance parameters as a function of device absorber bandgap energy (from EQE spectrum).

E_g [eV]	PCE [%]	V_{oc} [mV]	J_{sc} [mA cm^{-2}]	FF [%]	Sensitizing dye	Refs.
1.65	4.1	770	9.9	53.9	N719	[2]
1.74	4.6	750	10.5	58.0	N719	[2]
1.75	7.6	732	15.0	69.2	N719	[2][a]
1.78	7.5	725	15.4	67.5	N719	[2]
1.79	6.5	729	13.2	68.0	N719	[2]
1.80	6.3	732	13.1	66.0	N719	[2]
1.81	6.3	754	12.3	67.9	(JH-1)$_{0.6}$(SQ2)$_{0.4}$	[2]
183	5.0	735	10.0	67.8	N719	[2]
1.88	6.0	750	11.2	71.0	N719	[2]
1.90	4.2	680	10.7	57.7	N719	[2]
1.94	4.2	710	10.3	57.2	N719	[2]
1.95	4.9	702	11.2	62.3	N719	[2]
2.02	3.9	720	11.9	45.2	**N719**	[129]
2.12	5.4	680	10.4	76.3	N719	[2]

[a]Certified efficiency.

Table 14. Flexible monolithic multijunction research solar cells with the highest efficiency: performance parameters as a function of photovoltaic bandgap energies (from EQE spectrum) of each subcell.

$E_{g,bottom}$ [eV]	$E_{g,top}$ [eV]	PCE [%]	V_{oc} [mV]	J_{sc} [mA cm^{-2}]	FF [%]	Bottom absorber material	Top absorber material(s)	Refs.
1.00	**1.41, 1.91**[a]	**30.2**[b]	**3043**	**16.1**	**84.5**	**Ga$_{0.73}$In$_{0.27}$As**	**GaAs, Ga$_{0.51}$In$_{0.49}$P**[a]	[43]
1.25	**1.78**	**24.7**	**2000**	**15.8**	**78.3**	**FA$_{0.7}$MA$_{0.3}$Pb$_{0.5}$Sn$_{0.5}$I$_3$**	**FA$_{0.8}$Cs$_{0.2}$PbI$_{1.95}$Br$_{1.05}$**	[41]
1.25	**1.78**	**24.4**	**2016**	**15.6**	**77.3**	**FA$_{0.7}$MA$_{0.3}$Pb$_{0.5}$Sn$_{0.5}$I$_3$**	**FA$_{0.8}$Cs$_{0.2}$PbI$_{1.95}$Br$_{1.05}$**	[41][c]
1.26	**1.79**	**23.8**	**2.1**	**15.1**	**75.1**	**FA$_{0.6}$MA$_{0.4}$Pb$_{0.4}$Sn$_{0.6}$I$_3$**	**Cs$_{0.12}$FA$_{0.8}$MA$_{0.08}$PbI$_{1.8}$Br$_{1.2}$**	[130]
1.28	1.73	21.3	1820	15.6	75.0	FA$_{0.75}$Cs$_{0.25}$Sn$_{0.5}$Pb$_{0.5}$I$_3$	FA$_{0.6}$Cs$_{0.3}$DMA$_{0.1}$PbI$_{2.4}$Br$_{0.6}$	[2]
1.40	1.82	13.6	1800	11.1	68.3	PBDB-T:SN6IC-4F	Cs$_{0.1}$FA$_{0.54}$MA$_{0.36}$PbI$_{1.8}$Br$_{1.2}$	[2]
1.41	1.86	30.4	2547	14.3	84.7	GaAs	InGaP	[2]
1.41	1.92	27.4	2400	13.1	88.0	GaAs	InGaP	[2]

[a]For triple junction devices the middle and top subcell values are listed; [b]J–V measured under AM0 136.7 mW cm^{-2}; [c]Certified efficiency.

Table 15. Flexible single junction research solar cells with the highest efficiency: performance parameters as a function of device absorber bandgap energy (from EQE spectrum) among emerging inorganic technologies.

E_g [eV]	PCE [%]	V_{oc} [mV]	J_{sc} [mA cm^{-2}]	FF [%]	Absorber material	Refs.
1.04	**4.4**	**394**	**23.9**	**46.4**	**Cu$_2$Cd$_x$Zn$_{1-x}$Sn(S,Se)$_4$**	[131]
1.07	**4.9**	**358**	**28.7**	**47.3**	**Cu$_2$ZnSn(S,Se)$_4$**	[132]
1.13	**10.2**	**463**	**35.7**	**62.0**	**Cu$_2$ZnSn(S,Se)$_4$**	[133]
1.16	11.2	539	33.1	62.8	Cu$_2$ZnSn(S,Se)$_4$	[2]
1.32	6.13	415	25.5	57.9	Sb$_2$Se$_3$	[2]
1.52	0.6	204	7.6	35.5	Cu$_2$ZnSnS$_4$	[2]
1.59	**6.5**	**601**	**22.6**	**48.0**	**CZTSSe**	[134]

Table 16. Flexible single junction research solar cells with the highest efficiency: performance parameters as a function of device absorber bandgap energy (from EQE spectrum) among established inorganic technologies.

E_g [eV]	PCE [%]	V_{oc} [mV]	J_{sc} [mA cm^{-2}]	FF [%]	Absorber material/ technology	Refs.
1.11	**11.5**	**526**	**33.8**	**64.6**	**CIGSSe**	[135]
1.14	17.0	656	36.6	70.8	Si	[2]
1.17	18.9	608	39.5[135]	63.0	Si	[2]
1.17	12.0	580	35.8	58.4	CIGS	[2]
1.20	20.4	736	35.1	78.9	CIGS	[2][a]
1.22	18.7	720	35.0	74.4	CIGS	[2]
1.32	8.4	550	24.3	63.0	Si	[2]
1.42	22.1	980	27.1	83.4	GaAs	[2]
1.45	**13.5**	**786**	**22.1**	**77.7**	**GaAs**	[136]
1.46	14.1	821	24.334	70.3	CdTe	[137][a]
1.46	16.4	831	25.5	77.4	CdTe	[2]
1.49	11.5	821	22.0	63.9	CdTe	[2]
1.79	8.8	888	14.3	70	a-Si:H	[2]
1.88	8.2	820	15.6	64.0	a-Si:H	[2]

[a]Certified power conversion efficiency.

7.3. Best Performing Transparent and Semitransparent Research Solar Cells Tables

Data on best performing transparent and semitransparent research solar cells are given in **Tables 17–22**.

7.4. Operational Stability Tables of Emerging Research Solar Cells

Tables 23–26 present the summary of the experimental data on emerging research solar cells.

Table 17. Transparent/semitransparent perovskite research solar cells with the highest efficiency: performance parameters as a function of AVT and the photovoltaic bandgap energy (from EQE spectrum).

AVT [%]	E_g [eV]	PCE [%]	V_{oc} [mV]	J_{sc} [mA cm^{-2}]	FF [%]	Absorber	Refs.
3	**1.67**	**16.3**	**1099**	**18.9**	**78.3**	**Cs$_{0.25}$FA$_{0.75}$PbBr$_{0.6}$I$_{2.4}$**	[138]
3	1.64	15.7	1070	19.0	77.2	Cs$_{0.175}$FA$_{0.75}$MA$_{0.075}$PbBr$_{0.375}$I$_{2.625}$	[2]
3	1.53	12.2	1017	17.5	68.5	MAPbI$_3$	[2]
4	1.63	18.2	1076	21.1	80.0	CsFAMAPb(BrI)$_3$	[2]
5	**1.60**	**19.1**	**1120**	**23.2**	**73.4**	**MAPbI$_3$**	[139]
5	1.60	16.5	1080	20.6	74.2	MAPbI$_3$	[2]
5	1.61	12.0	960	19.2	65.3	MAPbCl$_x$I$_{3-x}$	[2]
5	1.65	11.2	940	18.4	64.9	MAPbI$_3$	[2]
6	1.60	15.8	1100	19.3	74.4	MAPbI$_3$	[2]
7	1.55	13.6	988	20.4	67.5	MAPbI$_3$	[2]
8	1.52	19.8	1137	21.9	79.5	Cs$_{0.05}$FA$_{0.95}$PbI$_3$	[2]
9	**1.63**	**17.8**	**1120**	**19.3**	**82.7**	**Cs$_{0.13}$FA$_{0.87}$PbBr$_{0.39}$I$_{2.61}$**	[140]
9	1.64	17.4	1083	21.5	75.1	Cs$_{0.175}$FA$_{0.825}$PbBr$_{0.375}$I$_{2.625}$	[2]
10	1.59	17.5	1070	22.4	73.1	MAPbI$_3$	[2]
10	1.65	16.1	1060	20.4	74.5	Cs$_{0.05}$FA$_{0.8075}$MA$_{0.1425}$PbBr$_{0.45}$I$_{2.55}$	[2]
12	1.60	13.2	1000	19.5	67.8	MAPbI$_3$	[2]
13	1.67	14.9	1100	19.8	68.4	MAPbBr$_{0.5}$I$_{2.5}$	[2]
13	**1.88**	**13.2**	**1298**	**13.8**	**74.1**	**Cs$_{0.25}$FA$_{0.75}$PbBr$_{1.5}$I$_{1.5}$**	[45]
14	1.64	13.6	1048	16.5	78.6	Cs$_{0.175}$FA$_{0.825}$PbBr$_{0.375}$I$_{2.875}$	[2]
14	1.57	13.0	970	19.1	69.9	MAPbI$_{3-x}$Cl$_x$	[2]
15	**1.64**	**11.4**	**1094**	**16.8**	**62.0**	**Cs$_{0.05}$FA$_{0.775}$MA$_{0.1615}$PbBr$_{0.51}$I$_{2.49}$**	[141]

**ADVANCED
SCIENCE NEWS**

www.advancedsciencenews.com

**ADVANCED
ENERGY
MATERIALS**

www.advenergymat.de

Table 17. Continued.

AVT [%]	E_g [eV]	PCE [%]	V_{oc} [mV]	J_{sc} [mA cm^{-2}]	FF [%]	Absorber	Refs.
15	1.61	11.9	1000	17.8	66.3	MAPbI$_3$	[2]
16	1.76	13.7	1120	16.7	73.4	MAPbBrI$_2$	[2]
17	1.65	12.8	1040	16.6	74.1	Cs$_{0.05}$FA$_{0.8075}$MA$_{0.1425}$PbBr$_{0.45}$I$_{2.55}$	[2]
18	1.77	12.2	1110	15.1	72.7	MAPbBrI$_2$	[2]
18	1.53	9.1	1017	14.6	61.5	MAPbI$_3$	[2]
19	1.55	8.8	941	13.7	68.3	MAPbI$_3$	[2]
20	1.63	11.7	1080	14.5	74.6	MAPbI$_3$ + BiPy-I	[2]
20	1.63	14.7	1108	17.6	75.2	K$_x$Cs$_{0.05}$FA$_{0.8075}$MA$_{0.1425}$PbBr$_{0.45}$I$_{2.55}$	[2]
21	1.63	14.2	1117	17.4	73.2	K$_x$Cs$_{0.05}$FA$_{0.8075}$MA$_{0.1425}$PbBr$_{0.45}$I$_{2.55}$	[2]
22	1.61	13.2	1073	17.2	71.7	K$_x$Cs$_{0.05}$FA$_{0.8075}$MA$_{0.1425}$PbBr$_{0.45}$I$_{2.55}$	[2]
23	1.61	12.3	1082	17.1	66.6	K$_x$Cs$_{0.05}$FA$_{0.8075}$MA$_{0.1425}$PbBr$_{0.45}$I$_{2.55}$	[2]
23	1.62	11.3	1040	15.1	72.3	MAPbI$_3$	[2]
23	1.57	10.8	970	17.3	64.4	MAPbCl$_x$I$_{3-x}$	[2]
23	**1.88**	**8.6**	**1236**	**10.0**	**69.9**	**Cs$_{0.25}$FA$_{0.75}$PbBr$_{1.5}$I$_{1.5}$**	**[45]**
24	1.87	9.4	1120	13.6	61.6	MAPbBr$_{1.5}$I$_{1.5}$	[2]
25	1.55	10.8	950	16.3	69.7	MAPbI$_3$	[2]
26	1.63	10.2	1070	12.2	78.1	MAPbI$_3$	[2]
27	1.60	12.1	1000	18.3	66.2	MAPbI$_3$	[2]
28	1.60	8.5	964	13.1	66.8	MAPbCl$_x$I$_{3-x}$	[2]
28	1.57	8.1	1030	11.2	70.2	MAPbCl$_x$I$_{3-x}$	[2]
30	1.62	12.8	1030	16.5	74.9	MAPbCl$_x$I$_{3-x}$	[2]
30	1.65	7.4	1010	11.8	62.2	Cs$_{0.05}$FA$_{0.8075}$MA$_{0.1425}$PbBr$_{0.45}$I$_{2.55}$	[2]
31	1.69	11.9	1050	16.3	69.4	MAPbBr$_{0.5}$I$_{2.5}$	[2]
33	1.55	7.3	1037	13.4	52.5	MAPbI$_3$	[2]
34	1.62	11.7	990	15.9	74.6	MAPbCl$_x$I$_{3-x}$	[2]
35	**1.88**	**12.0**	**1289**	**12.9**	**72.3**	**Cs$_{0.25}$FA$_{0.75}$PbBr$_{1.5}$I$_{1.5}$**	**[45]**
36	1.79	10.3	1080	14.6	65.5	MAPbBr I$_2$	[2]
37	1.62	10.8	1010	14.7	73.1	MAPbCl$_x$I$_{3-x}$	[2]
37	1.57	7.8	970	11.6	69.6	MAPbCl$_x$I$_{3-x}$	[2]
38	1.63	10.7	1060	13.0	77.6	MAPbI$_3$	[2]
41	1.90	8.8	1110	12.8	62.2	MAPbBr$_{1.5}$I$_{1.5}$	[2]
42	1.63	10.3	1000	13.6	75.6	MAPbCl$_x$I$_{3-x}$	[2]
45	1.64	8.5	960	12.6	73.5	MAPbCl$_x$I$_{3-x}$	[2]
46	1.57	3.6	1030	5.4	64.4	MAPbCl$_x$I$_{3-x}$	[2]
47	1.63	4.5	880	8.2	63.0	MAPbI$_3$	[2]
52	**1.88**	**4.1**	**1125**	**5.8**	**63.0**	**Cs$_{0.25}$FA$_{0.75}$PbBr$_{1.5}$I$_{1.5}$**	**[45]**
66	2.62	1.1	1000	2.1	52.9	Cs$_2$AgBiBr$_6$	[2]
68	2.35	7.8	1550	6.7	72.0	FAPbBr$_{2.43}$Cl$_{0.57}$	[2]
72	2.62	1.5	960	2.1	74.3	Cs$_2$AgBiBr$_6$	[2]
72	3.03	0.2	1110	0.6	35.4	MAPbCl$_3$	[2]
73	2.62	1.6	970	2.2	73.1	Cs$_2$AgBiBr$_6$	[2]
73	2.84	0.5	1260	0.9	44.9	MAPbBr$_{0.6}$Cl$_{2.4}$	[2]
74	2.62	1.5	970	2.2	71.1	Cs$_2$AgBiBr$_6$	[2]

Table 18. Transparent/semitransparent organic research solar cells with the highest efficiency: performance parameters as a function of AVT and the photovoltaic bandgap energy (from EQE spectrum).

AVT [%]	E_g [eV]	PCE [%]	V_{oc} [mV]	J_{sc} [mA cm^{-2}]	FF [%]	Active material	Refs.
1	1.40	13.3	810	24.6	66.5	PM6:Y6	[2]
2	1.66	7.6	770	15.6	63.3	PBDTTT-C-T:PC$_{71}$BM	[2]
3	1.40	12.6	800	24.5	64.5	PM6:Y6	[2]
6	1.47	12.0	870	19.6	70.4	PM7/PTTtID-Cl/IT-4F	[2]
8	**1.41**	**12.7**	**852**	**21.1**	**70.4**	**D18-Cl:Y6:PC$_{71}$BM**	**[142]**
9	1.42	14.2	854	23.0	72.3	PM6:Y6	[2]
11	1.66	7.1	760	14.5	64.4	PBDTTT-C-T:PC$_{71}$BM	[2]
13	1.42	13.3	853	21.7	71.9	PM6:Y6	[2]
14	1.40	13.6	850	21.1	75.8	PM6:Y6	[2]
14	1.41	12.0	844	19.6	72.8	PM6:Y6:C6	[2]
15	1.52	8.9	772	18.3	63.0	PTB7-Th:FNIC1	[2]
16	1.95	2.9	540	9.7	55.4	P3HT-PCBM	[2]
17	1.39	12.6	810	21.2	73.2	PBDB-T-2F:Y6	[2]
18	1.39	11.7	810	20.7	69.6	PBDB-T-2F:Y6	[2]
19	**1.42**	**13.6**	**830**	**23.4**	**70.2**	**PM6:Y7**	**[143]**
19	1.42	12.4	852	20.4	71.4	PM6:Y6	[2]
20	**1.37**	**14.0**	**820**	**23.0**	**74.3**	**PM6:Y6:SN3**	**[144]**
20	**1.39**	**14.6**	**860**	**22.8**	**74.7**	**PM6/ICBA:Y6**	**[145]**
20	1.42	12.3	817	20.6	73.0	PM6:Y6	[2]
20	**1.23**	**11.6**	**661**	**25.6**	**68.2**	**BTB7-Th:ATT-9**	**[27]**
21	**1.39**	**16.1**	**859**	**24.6**	**76.1**	**PM6-Ir1:BTP-eC9:PC$_{71}$BM**	**[146]**
21	1.41$^{a)}$	13.8	820	25.3	66.5	PM6:N3	[2]
25	1.34	11.0	750	20.9	70.0	PCE-10:A078	[2]
25	1.40	10.2	736	20.3	68.3	PTB7-Th:FOIC	[2]
25	**1.43**	**12.1**	**760**	**23.9**	**66.6**	**PM6:Y6**	**[147]**
26	1.40	12.9	825	21.6	72.4	PBDB-T-2F:Y6	[2]
28	**1.39**	**11.3**	**816**	**19.7**	**70.3**	**PM6:Y6-BO**	**[148]**
28	1.41 $^{a)}$	8.9	810	16.8	65.1	PM6:N3	[2]
28	1.66	5.6	760	11.9	61.9	PBDTTT-C-T:PC$_{71}$BM	[2]
29	1.41$^{a)}$	7.8	800	15.2	64. 7	PM6:N3	[2]
30	1.35	10.8	718	21.9	68.7	PTB7-Th:IEICO-4F	[2]
31	**1.39**	**12.0**	**758**	**22.8**	**69.5**	**PCE10-BDT2F-0.8:Y6**	**[149]**
32	**1.42**	**11.2**	**849**	**17.0**	**77.6**	**PM6:m-BTP-PhC6:BO-Cl**	**[150]**
34	1.40	9.1	733	18.5	67.1	PTB7-Th:FOIC	[2]
36	1.37	8.8	680	18.0	71.9	PCE-10:BT-CIC:TT-FIC	[2]
36	1.86	6.9	890	11.6	66.5	PSEHTT:ICBA	[2]
37	1.86	6.1	890	10.2	66.8	PSEHTT:ICBA	[2]
38	1.33	5.7	700	12.4	66.23	PTB7-Th:IEICO-4F	[2]
39	**1.41**	**13.0**	**849**	**19.0**	**80.3**	**PBDB-TF:L8-BO:BTP-eC9**	**[87]**
39	1.86	4.9	880	8.3	67.9	PSEHTT:ICBA	[2]
25	**1.43**	**9.7**	**770**	**20.0**	**63.0**	**PM6:Y6**	**[147]**
43	1.34	8.1	730	16.3	68.1	PCE-10:A078	[2]
44	1.37	8.0	680	16.2	72.6	PCE-10:BT-CIC:TT-FIC	[2]

Table 18. Continued.

AVT [%]	E_g [eV]	PCE [%]	V_{oc} [mV]	J_{sc} [mA cm^{-2}]	FF [%]	Active material	Refs.
46	1.34	10.8	750	20.4	70.6	PCE-10:A078	[2]
47	**1.39**	**11.4**	**854**	**18.0**	**74.5**	**PM6:BTP-eC9:L8-BO**	**[44]**
47	1.34	7.1	730	14.3	68.0	PCE-10:A078	[2]
47	1.86	2.4	860	4.1	68.2	PSEHTT:ICBA	[2]
49	1.37	7.2	670	14.8	72.6	PCE-10:BT-CIC:TT-FIC	[2]
50	1.38	8.3	746	16.7	66.8	PTB7-Th:FOIC:PC$_{71}$BM	[2]
51	1.39	7.4	749	14.7	66.7	PTB7:FOIC:PC71BM	[2]
53	1.86	1.8	890	3.8	54.8	PSEHTT:ICBA	[2]
53	1.32	5.7	750	10.6	69.5	DPP2T:IEICO-4F	[2]
60	1.33	3.9	749	7.34	70.2	DPP2T:IEICO-4F	[2]
62	1.33	5.9	690	12.9	66.0	PTB7-Th:6TIC-4F	[2]

[a] E_g taken from absorbance.

Table 19. Semitransparent/transparent dye sensitized research solar cells with the highest efficiency: performance parameters as a function of AVT and the photovoltaic bandgap energy (from EQE spectrum).

AVT [%]	E_g [eV]	PCE [%]	V_{oc} [mV]	J_{sc} [mA cm^{-2}]	FF [%]	Sensitizing dye	Refs.
1	2.00	5.2	780	12.4	53.7	N719	[2]
5	**1.80**	**11.0**	**871**	**16.8**	**75.2**	**C268 + Y1**	**[151]**
9	2.00	4.5	780	10.3	56.0	N719	[2]
9	1.82	4.3	720	9.9	60.0	N719 + SDA	[2]
10	2.01	5.2	770	11.9	57.0	N719	[2]
10	2.00	4.9	765	11.4	56.1	N719	[2]
10	**1.81**	**5.0**	**710**	**11.7**	**60.7**	**N719**	**[98]**
13	1.68	10.1	851	14.9	80.2	SGT-021	[2][a]
14	1.68	9.9	850	14.9	78.5	SGT-021	[2][a]
15	1.68	9.6	850	14.7	77.2	SGT-021	[2][a]
17	1.68	9.8	855	15.1	75.5	SGT-021	[2][a]
18	2.00	8.6	750	16.7	68.4	N719 (EtOH)	[2]
23	1.82	4.2	650	9.9	64.0	N719 + SDA	[2]
23	2.01	3.6	650	8.2	68.0	N719	[2]
24	2.00	7.8	794	17.4	56.3	N719 (EtOH)	[2]
25	1.82	2.6	650	5.6	71.0	N719 + SDA	[2]
27	1.77	3.7	521	10.7	65.8	NPI	[2]
30	2.19	1.5	640	3.3	70.0	N719	[2]
31	2.23	6.4	698	13.5	67.9	TPA-1 (EtOH)	[2]
33	2.30	6.1	711	12.5	68.3	TPA-2 (EtOH)	[2]
36	2.23	6.1	766	14.5	54.7	TPA-1 (EtOH)	[2]
37	2.46	3.5	648	8.0	67.5	Cz-2	[2]
38	2.31	5.7	769	13.6	54.2	TPA-2 (EtOH)	[2]
43	1.95	7.8	720	15.3	70.8	PdTPBP/BPEA	[2][b]
69	1.39	3.1	422	11.2	65.6	VG20-C$_{16}$	[2]
75	**1.53**	**2.5**	**408**	**10.9**	**56.2**	**TB207**	**[152]**
76	1.41	2.3	406	8.6	65.9	VG20-C$_{16}$	[2]

[a] Selective absorption-like EQE spectrum; [b] E_g calculated from transmittance spectrum.

Table 20. Semitransparent research solar cells with the highest efficiency among emerging inorganic technologies: performance parameters as a function of AVT and the photovoltaic bandgap energy (from EQE spectrum).

AVT [%]	E_g [eV]	PCE [%]	V_{oc} [mV]	J_{sc} [mA cm^{-2}]	FF [%]	Absorber/technology	Refs.
1	1.46	3.0	475	14.6	42.8	Cu$_2$ZnSn(S,Se)$_4$	[2]
8	1.83	3.4	679	12.1	42.0	Sb$_2$S$_3$	[2]

Table 21. Semitransparent research solar cells with the highest efficiency among established inorganic technologies: performance parameters as a function of AVT and the photovoltaic bandgap energy (from EQE spectrum).

AVT [%]	E_g [eV]	PCE [%]	V_{oc} [mV]	J_{sc} [mA cm^{-2}]	FF [%]	Absorber/ technology	Refs.
2	1.23	10.0	640	23.3	66.9	CIGS	[2]
5	1.26	9.8	630	22.9	67.6	CIGS	[2]
7	1.92	6.6	881	11.8	63.7	a-Si:H	[2]
9	1.30	9.8	630	20.9	74.1	CIGS	[2]
9	1.28	6.5	597	22.9	46.5	CIGS	[2]
11	1.34	8.4	620	20.4	66.3	CIGS	[2]
16	1.83	7.5	810	14.2	65.3	a-Si:H	[2]
17	1.83	7.7	810	14.1	67.3	a-Si:H	[2]
18	2.05	5.9	720	14.1	58.3	a-SiGe:H	[2]
18	1.50	5.9	710	14.6	57.4	CIGS	[2]
19	1.87	7.3	820	13.1	67.6	a-Si:H	[2]
19	1.30	6.9	640	16.6	64.7	CIGS	[2]
19	1.34	6.5	580	17.5	63.5	CIGS	[2]
20	1.64	1.7	495	8.9	40.8	CIGS	[2]
22	2.05	5.5	760	12.3	58.6	a-Si:H	[2]
23	1.92	6.0	830	10.6	68.2	a-Si:H	[2]
24	1.68[a]	6.9	920	10.7	70.3	a-Si:H	[2]
37	1.54	0.4	101	14.7	27.2	CdTe	[2]
45	2.16	1.1	596	3.9	47.3	a-Si:H	[2]

[a] E_g taken from absorption spectrum.

Table 22. Transparent photovoltaic devices with the highest efficiency including research solar cells with transparent luminescent solar concentrators: performance parameters (measured under the standard of Yang et al.)[46,47] as a function of the average visible transmittance and bandgap energy (from EQE spectrum).

AVT [%]	E_g [eV]	PCE [%]	V_{oc} [mV]	J_{sc} [mA cm^{-2}]	FF [%]	Luminophore(s)/absorber	Refs.
74	1.50	1.2	990	1.5	81.3	CO$_l$8DFIC/GaAs	[153]
75	1.64	3.0	1020	3.8	77.7	Cs$_2$Mo$_6$I$_8$(CF$_3$CF$_2$COO)$_6$: BODIPY/GaAs	[48]
84	1.11	0.4	520	1.3	65.1	(TBA)$_2$Mo$_6$Cl$_{14}$/Si	[154]
86	1.52	0.4	500	1.2	66.7	Cy7-NHS/Si	[155]

Table 23. Most operationally stable perovskite research solar cells in terms of the stability test energy yield for 200 and 1000 h under simulated 1 sun illumination as a function of the device bandgap energy (from EQE spectrum).

E_g [eV]	0 h PCE [%]	200 h PCE [%]	1000 h PCE [%]	E_{200h} [Wh cm^{-2}]	E_{1000h} [Wh cm^{-2}]	Absorber	Comments	Refs.
1.40	**9.4**	**9.4**	**9.2**	**1.9**	**9.3**	FASnI$_3$+NaBH$_4$+DipI	**MPP, AM1.5G, N$_2$, 70 °C**	[49,156]
1.45	**13.8**	**14.1**	**13.0**	**2.8**	**13.6**	**FASnI$_3$**	**MPP, AM1.5G, air**	[53]
1.53	23.5	20.9	–	4.3	–	α-FAPbI$_3$	MPP, w-LED, N$_2$, 35 °C	[2]
1.53	**23.1**	**22.7**	**20.7**	**4.6**	**22.0**	**FA$_{0.97}$MA$_{0.03}$PbI$_{2.91}$Br$_{0.09}$**	**MPP, AM1.5G, N$_2$, 40 °C**	[55]
1.54	23.02	20.9	19.4	4.3	20.4	FAPbI$_3$/FGCs	MPP, AM1.5G, N$_2$, 60 °C	[2]
1.57	21.8	22.0	21.8	4.2	22.0	Cs$_{0.05}$FA$_{0.874}$MA$_{0.076}$PbBr$_{0.24}$I$_{2.76}$	MPP, AM1.5G, N$_2$, 40 °C, UV-f	[2]
1.57	20.6	20.2	20.2	4.1	20.1	FA$_x$Cs$_{1-x}$PbI$_3$	MPP, w-LED, Ar, 55–60 °C	[2]
1.57	**19.8**	**20.6**	**17.7**	**4.1**	**19.1**	**FA$_{0.95}$MA$_{0.05}$PbBr$_{0.15}$I$_{2.85}$**	**MPP, w-LED, air, 55 °C**	[60]
1.58	**23.1**	**22.9**	**–**	**4.6**	**–**	**Cs$_{0.05}$FA$_{0.9}$MA$_{0.05}$ Pb Br$_{0.26}$I$_{2.74}$**	**MPP, N$_2$**	[19]
1.58	**23.6**	**20.2**	**–**	**4.4**	**–**	**FA$_{0.92}$MA$_{0.08}$PbBr$_{0.24}$I$_{2.76}$**	**MPP, AM1.5G, air, 50% RH**	[157]
1.58	19.2	19.3	18.4	3.9	19.0	Cs$_{0.05}$FA$_{0.7885}$MA$_{0.1615}$PbBr$_{0.3}$I$_{2.7}$	OC, AM1.5G, encapsulation, 70–75 °C	[2]
1.59	17.1	11.6	9.5	2.8	11.1	Gua$_{0.15}$MA$_{0.85}$PbI$_3$	MPP, AM1.5G, Ar, 60 °C	[2]
1.60	21.8	21.4	19.8	4.3	20.9	CsMAFAPbI$_3$:PPP	MPP, encapsulation, air, AM1.5G, 75 °C	[2]
1.60	21.3	21.1	21.3	4.2	21.2	CsFAMAPbI$_3$:PPP	MPP, encapsulation, air, AM1.5G, 45 °C	[2]
1.60	19.6	19.6	18.8	3.9	19.4	Cs$_{0.05}$FA$_{0.81}$MA$_{0.14}$PbBr$_{0.45}$I$_{2.55}$	MPP-R$_L$, AM1.5G, encapsulation, 50–70% RH, 65 °C	[2]
1.60	**19.6**	**18.4**	**16.3**	**3.8**	**17.4**	**CsFAMAPbBrI**	**MPP, AM1.5G, air, 40% RH, 30 °C**	[122]
1.61	18.1	11.9	13.6	2.6	13.0	Gua$_{0.25}$MA$_{0.75}$PbI$_3$	MPP, AM1.5G, Ar, 60 °C	[2]
1.62	21.1	19.9	18.0	4.0	19.1	Cs$_{0.04}$FA$_{0.8064}$MA$_{0.1536}$PbBr$_{0.48}$I$_{2.52}$	MPP, AM1.5G, N$_2$, 40 °C	[2]
1.63	20.0	16.8	11.8[a]	3.5	15.1	Cs$_{0.05}$FA$_{0.79}$MA$_{0.16}$PbBr$_{0.51}$I$_{2.49}$	MPP, AM1.5G, N$_2$, 25 °C	[2]
1.63	21.0	19.7	19.4[a]	3.9	19.6	Cs$_{0.05}$FA$_{0.81}$MA$_{0.14}$PbBr$_{0.45}$I$_{2.55}$/FGCs	MPP, AM1.5G, N$_2$, 60 °C	[2]
1.64	20.1	17.8	–	3.7	–	Cs$_{0.1}$FA$_{0.747}$MA$_{0.153}$PbBr$_{0.51}$I$_{2.49}$	MPP, w-LED, N$_2$, 25 °C	[2]
1.64[b]	19.7	17.2	–	3.5	–	Cs$_{0.5}$FA$_{0.7885}$MA$_{0.1615}$PbBr$_{0.51}$I$_{2.49}$	MPP, w-LED, N$_2$, 20 °C	[2]
1.66	13.0	14.7	13.0	2.8	14.1	Cs$_{0.17}$FA$_{0.83}$PbBr$_{0.51}$I$_{2.49}$	MPP, AM1.5G, 40% RH, 35 °C	[2]
1.69	6.8	6.7	–	1.3	–	CsGe$_{0.5}$Sn$_{0.5}$I$_3$	MPP, AM1.5G, N$_2$, 45 °C	[2]
1.74	12.9	13.4	–	2.7	–	CsPbI$_3$	OC, AM1.5G, N$_2$, 25 °C, UV-f	[2]

[a]Extrapolated value; [b]E_g taken from PL peak; abbreviations: MPP, maximum power point (tracking during test); OC, open-circuit (condition during test); UV-f, ultraviolet light filter; w-LED, white light spectrum light emitting diode source; RH, relative humidity; MPP-R$_L$, the cell is connected to the load resistance which matches the initial maximum power point.

Table 24. Most operationally stable organic research solar cells in terms of the stability test energy yield for 200 and 1000 h under simulated 1 sun illumination as a function of the device bandgap energy (from EQE spectrum).

E_g [eV]	0 h PCE [%]	200 h PCE [%]	1000 h PCE [%]	E_{200h} [Wh cm^{-2}]	E_{1000h} [Wh cm^{-2}]	Active material	Comments	Refs.
1.56	7.8	7.2	6.8	1.5	7.0	PBDB-T:ITIC-2F	OC, w-LED, N$_2$, 40 °C, UV-f	[2]
1.57	5.0	5.0	4.7	1.0	4.8	P3HT:o-IDTBR	OC, AM1.5G, N$_2$, UV-f	[2]
1.61	5.1	4.9	4.9	1.1	4.9	Dyad 4	OC, w-LED, N$_2$, 30 °C	[2]
1.66	8.0	7.4	7.0	1.5	7.3	PBDB-T:ITIC-Th	OC, w-LED, N$_2$, 40 °C, UV-f	[2]
1.70	8.7	8.1	-	1.6	-	PBDB-T:IDTBR	OC, AM1.5G, N$_2$, 35—40 °C	[2]
1.84	5.9	5.6	5.4	1.1	5.6	PBDB-T:PCBM	OC, w-LED, N$_2$, 40 °C, UV-f	[2]
1.94	3.7	3.7	3.7	0.7	3.7	P3HT-PCBM	OC, AM1.5G, air	[2]

Abbreviations: OC, open-circuit (condition during test); UV-f, ultraviolet light filter; w-LED, white light spectrum light emitting diode source.

Table 25. Most operationally stable dye-sensitized research solar cells in terms of the stability test energy yield for 200 and 1000 h under simulated 1 sun illumination as a function of the device bandgap energy (from EQE spectrum).

E_g [eV]	0 h PCE [%]	200 h PCE [%]	1000 h PCE [%]	E_{200h} [Wh cm^{-2}]	E_{1000h} [Wh cm^{-2}]	Sensitizing dye	Comments	Refs.
1.59	9.0	9.0	8.2	1.8	8.7	TF-tBu_C3F7	OC, AM1.5G, 65 °C	[2]
1.75	6.5	6.7	6.3	1.4	6.6	N719	OC, AM1.5G, 35 °C, UV-f	[2]
1.77	6.3	5.8	4.8	1.3	5.5	Z907	OC, w-LED, 20 °C	[2]
1.78	9.3	9.9	7.9	1.9	9.2	N719	OC, AM1.5G, 50 °C	[2]
1.83	8.4	8.3	–	1.7	–	MK2	OC, w-LED	[2]
1.85	8.0	8.3	8.3	1.4	8.1	N719	OC, AM1.5G	[2]
2.07	5.8	6.5	5.9	1.3	6.2	D35	OC, AM1.5G, 60 °C	[2]

Abbreviations: OC, open-circuit (condition during test); UV-f, ultraviolet light filter; w-LED, white light spectrum light emitting diode source.

Table 26. Most operationally stable multijunction research solar cells in terms of the stability test energy yield for 200 and 1000 h under simulated/ equivalent 1 sun illumination as a function of the device bandgap energies (from EQE spectra) of the absorber materials.

Bottom E_g [eV]	Top E_g [eV]	0 h PCE [%]	200 h PCE [%]	1000 h PCE [%]	E_{200h} [Wh cm^{-2}]	E_{1000h} [Wh cm^{-2}]	Bottom absorber material	Top absorber material	Comments	Refs.
						Perovskite/perovskite				
1.25	**1.80**	**25.6**	**26.4**	**17.8**	**5.2**	**23.5**	**$FA_{0.8}Cs_{0.2}Pb(I_{0.62}Br_{0.38})_3$**	**$FA_{0.7}MA_{0.3}Pb_{0.5}Sn_{0.5}I_3$**	**MPP, AM1.5G, air 30–50% RH, 35 °C**	**[36]**
1.26	1.82	24.4	24.3	19.3[a]	4.9	21.8[a]	$FSA{:}MA_{0.3}FA_{0.7}Pb_{0.5}Sn_{0.5}I_3$	$FA_{0.8}Cs_{0.2}Pb(I_{0.6}Br_{0.4})_3$	MPP, encapsulation, air, 30–50% RH, AM1.5G, no UV-f, 54–60 °C	[2]
1.26	1.82	21.2	20.6	19.8	4.2	20.7	$Cs_{0.05}MA_{0.45}FA_{0.5}Pb_{0.5}Sn_{0.5}I_3$	$Cs_{0.4}FA_{0.6}PbI_{1.95}Br_{1.05}$	MPP-R_L, encapsulation, air, AM1.5G, room temperature	[2]
1.27	1.72	23.1	22.2	20.4	4.7	21.4	$(FASnI_3)_{0.6}(MAPbI_3)_{0.4}$	$Cs_{0.05}FA_{0.8}MA_{0.15}PbI_{2.55}Br_{0.45}$	MPP, AM1.5G	[2]
						GaAs/perovskite				
1.42	1.85	24.1	23.9	22.1[a]	4.76	23.3[a]	GaAs	$FA_{0.80}MA_{0.04}Cs_{0.16}Pb(I_{0.50}Br_{0.50})_3$	MPP, air 20–25% RH, AM1.5G, room T, UV-f	[2]
						CIGS/perovskite				
1.10	1.65	22.0	19.9	18.4[a]	4.1	19.4[a]	CIGS	$Cs_{0.09}FA_{0.77}MA_{0.14}Pb(I_{0.86}Br_{0.14})_3$	MPP, air 20% RH, 30 °C	[2]

[a]Extrapolated value; abbreviations: MPP, maximum power point (tracking during test); UV-f, ultraviolet light filter; RH, relative humidity; MPP-R_L, the cell is connected to the load resistance which matches the initial maximum power point.

Supporting Information

Supporting Information is available from the Wiley Online Library or from the author.

Conflict of Interest

R.R.L. is a co-founder, director, and a part owner of Ubiquitous Energy, Inc., a company working to commercialize transparent photovoltaic technologies. All other authors declare no competing financial interest.

[1] O. Almora, D. Baran, G. C. Bazan, C. Berger, C. I. Cabrera, K. R. Catchpole, S. Erten-Ela, F. Guo, J. Hauch, A. W. Y. Ho-Baillie, T. J. Jacobsson, R. A. J. Janssen, T. Kirchartz, Y. Li, M. A. Loi, R. R. Lunt, X. Mathew, M. D. McGehee, J. Min, D. B. Mitzi, M. K. Nazeeruddin, J. Nelson, A. F. Nogueira, U. W. Paetzold, N.-G. Park, B. P. Rand, U. Rau, H. J. Snaith, E. Unger, L. Vaillant-Roca, et al., *Adv. Energy Mater.* **2021**, *11*, 2002774.

[2] O. Almora, D. Baran, G. C. Bazan, C. Berger, C. I. Cabrera, K. R. Catchpole, S. Erten-Ela, F. Guo, J. Hauch, A. W. Y. Ho-Baillie, T. J. Jacobsson, R. A. J. Janssen, T. Kirchartz, N. Kopidakis, Y. Li, M. A. Loi, R. R. Lunt, X. Mathew, M. D. McGehee, J. Min, D. B. Mitzi, M. K. Nazeeruddin, J. Nelson, A. F. Nogueira, U. W. Paetzold, N.-G. Park, B. P. Rand, U. Rau, H. J. Snaith, E. Unger, et al., *Adv. Energy Mater.* **2021**, *11*, 2102526.

[3] M. A. Green, E. D. Dunlop, J. Hohl-Ebinger, M. Yoshita, N. Kopidakis, K. Bothe, D. Hinken, M. Rauer, X. Hao, *Prog. Photovoltaics* **2022**, *30*, 687.

[4] W. Shockley, H. J. Queisser, *J. Appl. Phys.* **1961**, *32*, 510.

[5] A. S. Brown, M. A. Green, in *Conf. Record of the Twenty-Ninth IEEE Photovoltaic Specialists Conf.*, IEEE, New Orleans, LA, USA **2002**, pp. 868–871, https://doi.org/10.1109/PVSC.2002.1190717.

[6] A. S. Brown, M. A. Green, *Phys. Educ.* **2002**, *14*, 96.

[7] O. Almora, C. I. Cabrera, J. Garcia-Cerrillo, T. Kirchartz, U. Rau, C. J. Brabec, *Adv. Energy Mater.* **2021**, *11*, 2100022.

[8] L. Krückemeier, U. Rau, M. Stolterfoht, T. Kirchartz, *Adv. Energy Mater.* **2020**, *10*, 1902573.

[9] A. S. Brown, M. A. Green, *Phys. E* **2002**, *14*, 96.

[10] J.-F. Guillemoles, T. Kirchartz, D. Cahen, U. Rau, *Nat. Photonics* **2019**, *13*, 501.

[11] C. Yang, D. Liu, M. Bates, M. C. Barr, R. R. Lunt, *Joule* **2019**, *3*, 1803.

[12] C. J. Traverse, R. Pandey, M. C. Barr, R. R. Lunt, *Nat. Energy* **2017**, *2*, 849.

[13] S. Rühle, *Sol. Energy* **2016**, *130*, 139.

[14] Y. Ren, D. Zhang, J. Suo, Y. Cao, F. T. Eickemeyer, N. Vlachopoulos, S. M. Zakeeruddin, A. Hagfeldt, M. Grätzel, *Nature* **2022**, https://doi.org/10.1038/s41586-022-05460-z.

[15] Y. Zhao, S. Wang, C. Jiang, C. Li, P. Xiao, R. Tang, J. Gong, G. Chen, T. Chen, J. Li, X. Xiao, *Adv. Energy Mater.* **2022**, *12*, 2103015.

[16] Z. Sun, M. Liu, Y. Zhou, Q. Wang, Y. Yang, Y. Zhou, F. Liu, *Sol. Energy Mater. Sol. Cells* **2022**, *235*, 111453.

[17] M. Kim, J. Jeong, H. Lu, K. Lee Tae, T. Eickemeyer Felix, Y. Liu, W. Choi In, J. Choi Seung, Y. Jo, H.-B. Kim, S.-I. Mo, Y.-K. Kim, H. Lee, G. An Na, S. Cho, R. Tress Wolfgang, M. Zakeeruddin Shaik, A. Hagfeldt, Y. Kim Jin, M. Grätzel, S. Kim Dong, *Science* **2022**, *375*, 302.

[18] D. Grabowski, Z. Liu, G. Schöpe, U. Rau, T. Kirchartz, *Sol. RRL* **2022**, *6*, 2200507.

[19] J. Peng, F. Kremer, D. Walter, Y. Wu, Y. Ji, J. Xiang, W. Liu, T. Duong, H. Shen, T. Lu, F. Brink, D. Zhong, L. Li, O. Lee Cheong Lem, Y. Liu, K. J. Weber, T. P. White, K. R. Catchpole, *Nature* **2022**, *601*, 573.

[20] M. A. Mahmud, J. Zheng, S. Tang, G. Wang, J. Bing, A. D. Bui, J. Qu, L. Yang, C. Liao, H. Chen, S. P. Bremner, H. T. Nguyen, J. Cairney, A. W. Y. Ho-Baillie, *Adv. Energy Mater.* **2022**, *12*, 2201672.

[21] Z. Li, B. Li, X. Wu, S. A. Sheppard, S. Zhang, D. Gao, N. J. Long, Z. Zhu, *Science* **2022**, *376*, 416.

[22] Q. Jiang, J. Tong, Y. Xian, R. A. Kerner, S. P. Dunfield, C. Xiao, R. A. Scheidt, D. Kuciauskas, X. Wang, M. P. Hautzinger, R. Tirawat, M. C. Beard, D. P. Fenning, J. J. Berry, B. W. Larson, Y. Yan, K. Zhu, *Nature* **2022**, *611*, 278.

[23] Y. Lei, Y. Li, C. Lu, Q. Yan, Y. Wu, F. Babbe, H. Gong, S. Zhang, J. Zhou, R. Wang, R. Zhang, Y. Chen, H. Tsai, Y. Gu, H. Hu, Y.-H. Lo, W. Nie, T. Lee, J. Luo, K. Yang, K.-I. Jang, S. Xu, *Nature* **2022**, *608*, 317.

[24] X. Zhou, L. Zhang, J. Yu, D. Wang, C. Liu, S. Chen, Y. Li, Y. Li, M. Zhang, Y. Peng, Y. Tian, J. Huang, X. Wang, X. Guo, B. Xu, *Adv. Mater.* **2022**, *34*, 2205809.

[25] L. Zhu, M. Zhang, J. Xu, C. Li, J. Yan, G. Zhou, W. Zhong, T. Hao, J. Song, X. Xue, Z. Zhou, R. Zeng, H. Zhu, C.-C. Chen, R. C. I. MacKenzie, Y. Zou, J. Nelson, Y. Zhang, Y. Sun, F. Liu, *Nat. Mater.* **2022**, *21*, 656.

[26] Y. Wei, Z. Chen, G. Lu, N. Yu, C. Li, J. Gao, X. Gu, X. Hao, G. Lu, Z. Tang, J. Zhang, Z. Wei, X. Zhang, H. Huang, *Adv. Mater.* **2022**, *34*, 2204718.

[27] W. Liu, S. Sun, S. Xu, H. Zhang, Y. Zheng, Z. Wei, X. Zhu, *Adv. Mater.* **2022**, *34*, 2200337.

[28] J. Wang, J. Zhou, X. Xu, F. Meng, C. Xiang, L. Lou, K. Yin, B. Duan, H. Wu, J. Shi, Y. Luo, D. Li, H. Xin, Q. Meng, *Adv. Mater.* **2022**, *34*, 2202858.

[29] Y. C. Choi, D. U. Lee, J. H. Noh, E. K. Kim, S. I. Seok, *Adv. Funct. Mater.* **2014**, *24*, 3587.

[30] X. Wang, R. Tang, C. Jiang, W. Lian, H. Ju, G. Jiang, Z. Li, C. Zhu, T. Chen, *Adv. Energy Mater.* **2020**, *10*, 2002341.

[31] R. Tang, X. Wang, W. Lian, J. Huang, Q. Wei, M. Huang, Y. Yin, C. Jiang, S. Yang, G. Xing, S. Chen, C. Zhu, X. Hao, M. A. Green, T. Chen, *Nat. Energy* **2020**, *5*, 587.

[32] Y. Wang, S. R. Kavanagh, I. Burgués-Ceballos, A. Walsh, D. O. Scanlon, G. Konstantatos, *Nat. Photonics* **2022**, *16*, 235.

[33] NREL's Best Research-Cell Efficiency Chart, https://www.nrel.gov/pv/cell-efficiency.html (accessed: May 2020).

[34] M. A. Green, K. Emery, Y. Hishikawa, W. Warta, E. D. Dunlop, *Prog. Photovoltaics* **2012**, *20*, 12.

[35] M. A. Ruiz-Preciado, F. Gota, P. Fassl, I. M. Hossain, R. Singh, F. Laufer, F. Schackmar, T. Feeney, A. Farag, I. Allegro, H. Hu, S. Gharibzadeh, B. A. Nejand, V. S. Gevaerts, M. Simor, P. J. Bolt, U. W. Paetzold, *ACS Energy Lett.* **2022**, *7*, 2273.

[36] R. Lin, J. Xu, M. Wei, Y. Wang, Z. Qin, Z. Liu, J. Wu, K. Xiao, B. Chen, S. M. Park, G. Chen, H. R. Atapattu, K. R. Graham, J. Xu, J. Zhu, L. Li, C. Zhang, E. H. Sargent, H. Tan, *Nature* **2022**, *603*, 73.

[37] L. Mao, T. Yang, H. Zhang, J. Shi, Y. Hu, P. Zeng, F. Li, J. Gong, X. Fang, Y. Sun, X. Liu, J. Du, A. Han, L. Zhang, W. Liu, F. Meng, X. Cui, Z. Liu, M. Liu, *Adv. Mater.* **2022**, *34*, 2206193.

[38] J. Zheng, G. Wang, W. Duan, M. A. Mahmud, H. Yi, C. Xu, A. Lambertz, S. Bremner, K. Ding, S. Huang, A. W. Y. Ho-Baillie, *ACS Energy Lett.* **2022**, *7*, 3003.

[39] K. Xiao, J. Wen, Q. Han, R. Lin, Y. Gao, S. Gu, Y. Zang, Y. Nie, J. Zhu, J. Xu, H. Tan, *ACS Energy Lett.* **2020**, *5*, 2819.

[40] R. M. France, J. F. Geisz, T. Song, W. Olavarria, M. Young, A. Kibbler, M. A. Steiner, *Joule* **2022**, *6*, 1121.

[41] L. Li, Y. Wang, X. Wang, R. Lin, X. Luo, Z. Liu, K. Zhou, S. Xiong, Q. Bao, G. Chen, Y. Tian, Y. Deng, K. Xiao, J. Wu, M. I. Saidaminov, H. Lin, C.-Q. Ma, Z. Zhao, Y. Wu, L. Zhang, H. Tan, *Nat. Energy* **2022**, *7*, 708.

[42] G. Zeng, W. Chen, X. Chen, Y. Hu, Y. Chen, B. Zhang, H. Chen, W. Sun, Y. Shen, Y. Li, F. Yan, Y. Li, *J. Am. Chem. Soc.* **2022**, *144*, 8658.

[43] J. Schön, G. M. M. W. Bissels, P. Mulder, R. H. van Leest, N. Gruginskie, E. Vlieg, D. Chojniak, D. Lackner, *Prog. Photovoltaics* **2022**, *30*, 1003.

[44] X. Liu, Z. Zhong, R. Zhu, J. Yu, G. Li, *Joule* **2022**, *6*, 1918.

[45] J. C. Yu, B. Li, C. J. Dunn, J. Yan, B. T. Diroll, A. S. R. Chesman, J. J. Jasieniak, *Adv. Sci.* **2022**, *9*, 2201487.

[46] C. Yang, D. Liu, R. R. Lunt, *Joule* **2019**, *3*, 2871.

[47] C. Yang, H. A. Atwater, M. A. Baldo, D. Baran, C. J. Barile, M. C. Barr, M. Bates, M. G. Bawendi, M. R. Bergren, B. Borhan, C. J. Brabec, S. Brovelli, V. Bulović, P. Ceroni, M. G. Debije, J.-M. Delgado-Sanchez, W.-J. Dong, P. M. Duxbury, R. C. Evans, S. R. Forrest, D. R. Gamelin, N. C. Giebink, X. Gong, G. Griffini, F. Guo, C. K. Herrera, A. W. Y. Ho-Baillie, R. J. Holmes, S.-K. Hong, T. Kirchartz, et al., *Joule* **2022**, *6*, 8.

[48] C. Yang, W. Sheng, M. Moemeni, M. Bates, C. K. Herrera, B. Borhan, R. R. Lunt, *Adv. Energy Mater.* **2021**, *11*, 2003581.

[49] J. Sanchez-Diaz, R. S. Sánchez, S. Masi, M. Krečmarová, A. O. Alvarez, E. M. Barea, J. Rodriguez-Romero, V. S. Chirvony, J. F. Sánchez-Royo, J. P. Martinez-Pastor, I. Mora-Seró, *Joule* **2022**, *6*, 861.

[50] G. Kapil, T. Bessho, Y. Sanehira, S. R. Sahamir, M. Chen, A. K. Baranwal, D. Liu, Y. Sono, D. Hirotani, D. Nomura, K. Nishimura, M. A. Kamarudin, Q. Shen, H. Segawa, S. Hayase, *ACS Energy Lett.* **2022**, *7*, 966.

[51] Z. Zhu, X. Jiang, D. Yu, N. Yu, Z. Ning, Q. Mi, *ACS Energy Lett.* **2022**, *7*, 2079.

[52] Y. Su, J. Yang, G. Liu, W. Sheng, J. Zhang, Y. Zhong, L. Tan, Y. Chen, *Adv. Funct. Mater.* **2022**, *32*, 2109631.

[53] T. Wu, X. Liu, X. Luo, H. Segawa, G. Tong, Y. Zhang, L. K. Ono, Y. Qi, L. Han, *Nano-Micro Lett.* **2022**, *14*, 99.

[54] Z. Xiong, X. Chen, B. Zhang, G. O. Odunmbaku, Z. Ou, B. Guo, K. Yang, Z. Kan, S. Lu, S. Chen, N. A. N. Ouedraogo, Y. Cho, C. Yang, J. Chen, K. Sun, *Adv. Mater.* **2022**, *34*, 2106118.

[55] F. Zhang, Y. Park So, C. Yao, H. Lu, P. Dunfield Sean, C. Xiao, S. Uličná, X. Zhao, L. Du Hill, X. Chen, X. Wang, E. Mundt Laura, H. Stone Kevin, T. Schelhas Laura, G. Teeter, S. Parkin, L. Ratcliff Erin, Y.-L. Loo, J. Berry Joseph, C. Beard Matthew, Y. Yan, W. Larson Bryon, K. Zhu, *Science* **2022**, *375*, 71.

[56] Y. Zhao, F. Ma, Z. Qu, S. Yu, T. Shen, H.-X. Deng, X. Chu, X. Peng, Y. Yuan, X. Zhang, J. You, *Science* **2022**, *377*, 531.

[57] Y. Li, Z. Chen, B. Yu, S. Tan, Y. Cui, H. Wu, Y. Luo, J. Shi, D. Li, Q. Meng, *Joule* **2022**, *6*, 676.

[58] S. Tan, T. Huang, I. Yavuz, R. Wang, T. W. Yoon, M. Xu, Q. Xing, K. Park, D.-K. Lee, C.-H. Chen, R. Zheng, T. Yoon, Y. Zhao, H.-C. Wang, D. Meng, J. Xue, Y. J. Song, X. Pan, N.-G. Park, J.-W. Lee, Y. Yang, *Nature* **2022**, *605*, 268.

[59] Z. Shen, Q. Han, X. Luo, Y. Shen, T. Wang, C. Zhang, Y. Wang, H. Chen, X. Yang, Y. Zhang, L. Han, *Energy Environ. Sci.* **2022**, *15*, 1078.

[60] X. Li, W. Zhang, X. Guo, C. Lu, J. Wei, J. Fang, *Science* **2022**, *375*, 434.

[61] X. Wang, W. Sun, Y. Tu, Q. Xiong, G. Li, Z. Song, Y. Wang, Y. Du, Q. Chen, C. Deng, Z. Lan, P. Gao, J. Wu, *Chem. Eng. J.* **2022**, *446*, 137416.

[62] Y. Zhang, N.-G. Park, *ACS Energy Lett.* **2022**, *7*, 757.

[63] S. Wang, Y. Li, J. Yang, T. Wang, B. Yang, Q. Cao, X. Pu, L. Etgar, J. Han, J. Zhao, X. Li, A. Hagfeldt, *Angew. Chem., Int. Ed.* **2022**, *61*, 202116534.

[64] G. Yang, Z. Ni, Z. J. Yu, B. W. Larson, Z. Yu, B. Chen, A. Alasfour, X. Xiao, J. M. Luther, Z. C. Holman, J. Huang, *Nat. Photonics* **2022**, *16*, 588.

[65] S. Tan, B. Yu, Y. Cui, F. Meng, C. Huang, Y. Li, Z. Chen, H. Wu, J. Shi, Y. Luo, D. Li, Q. Meng, *Angew. Chem., Int. Ed.* **2022**, *61*, 202201300.

[66] J. Wen, Y. Zhao, Z. Liu, H. Gao, R. Lin, S. Wan, C. Ji, K. Xiao, Y. Gao, Y. Tian, J. Xie, C. J. Brabec, H. Tan, *Adv. Mater.* **2022**, *34*, 2110356.

[67] K. Xiao, Y.-H. Lin, M. Zhang, R. D. J. Oliver, X. Wang, Z. Liu, X. Luo, J. Li, D. Lai, H. Luo, R. Lin, J. Xu, Y. Hou, H. J. Snaith, H. Tan, *Science* **2022**, *376*, 762.

[68] S. Qin, C. Lu, Z. Jia, Y. Wang, S. Li, W. Lai, P. Shi, R. Wang, C. Zhu, J. Du, J. Zhang, L. Meng, Y. Li, *Adv. Mater.* **2022**, *34*, 2108829.

[69] Z. Guo, A. K. Jena, I. Takei, M. Ikegami, A. Ishii, Y. Numata, N. Shibayama, T. Miyasaka, *Adv. Funct. Mater.* **2021**, *31*, 2103614.

[70] W. Chen, D. Li, X. Chen, H. Chen, S. Liu, H. Yang, X. Li, Y. Shen, X. Ou, Y. Yang, L. Jiang, Y. Li, Y. Li, *Adv. Funct. Mater.* **2022**, *32*, 2109321.

[71] H. Xu, Z. Liang, J. Ye, S. Xu, Z. Wang, L. Zhu, X. Chen, Z. Xiao, X. Pan, G. Liu, *Chem. Eng. J.* **2022**, *437*, 135181.

[72] X. Li, Y. Tan, H. Lai, S. Li, Y. Chen, S. Li, P. Xu, J. Yang, *ACS Appl. Mater. Interfaces* **2019**, *11*, 29746.

[73] H. Zhu, L. Pan, F. T. Eickemeyer, M. A. Hope, O. Ouellette, A. Q. M. Alanazi, J. Gao, T. P. Baumeler, X. Li, S. Wang, S. M. Zakeeruddin, Y. Liu, L. Emsley, M. Grätzel, *ACS Energy Lett.* **2022**, *7*, 1112.

[74] X. Yao, B. He, J. Zhu, J. Ti, L. Cui, R. Tui, M. Wei, H. Chen, J. Duan, Y. Duan, Q. Tang, *Nano Energy* **2022**, *96*, 107138.

[75] J. Zhu, Y. Liu, B. He, W. Zhang, L. Cui, S. Wang, H. Chen, Y. Duan, Q. Tang, *Chem. Eng. J.* **2022**, *428*, 131950.

[76] H. Yuan, Y. Zhao, J. Duan, Y. Wang, X. Yang, Q. Tang, *J. Mater. Chem. A* **2018**, *6*, 24324.

[77] B. Li, X. Wu, S. Zhang, Z. Li, D. Gao, X. Chen, S. Xiao, C.-C. Chueh, A. K. Y. Jen, Z. Zhu, *Chem. Eng. J.* **2022**, *446*, 137144.

[78] Z. Liu, H.-E. Wang, *Sustainable Energy Fuels* **2022**, *6*, 744.

[79] Z. Liu, N. Wang, *Sol. Energy* **2021**, *214*, 110.

[80] Y. Pan, X. Zheng, J. Guo, Z. Chen, S. Li, C. He, S. Ye, X. Xia, S. Wang, X. Lu, H. Zhu, J. Min, L. Zuo, M. Shi, H. Chen, *Adv. Funct. Mater.* **2022**, *32*, 2108614.

[81] L. Zhan, S. Li, Y. Li, R. Sun, J. Min, Z. Bi, W. Ma, Z. Chen, G. Zhou, H. Zhu, M. Shi, L. Zuo, H. Chen, *Joule* **2022**, *6*, 662.

[82] Y. Cai, Y. Li, R. Wang, H. Wu, Z. Chen, J. Zhang, Z. Ma, X. Hao, Y. Zhao, C. Zhang, F. Huang, Y. Sun, *Adv. Mater.* **2021**, *33*, 2101733.

[83] D. Wang, G. Zhou, Y. Li, K. Yan, L. Zhan, H. Zhu, X. Lu, H. Chen, C.-Z. Li, *Adv. Funct. Mater.* **2022**, *32*, 2107827.

[84] T. Zhang, C. An, Y. Cui, J. Zhang, P. Bi, C. Yang, S. Zhang, J. Hou, *Adv. Mater.* **2022**, *34*, 2105803.

[85] L. Zuo, S. B. Jo, Y. Li, Y. Meng, R. J. Stoddard, Y. Liu, F. Lin, X. Shi, F. Liu, H. W. Hillhouse, D. S. Ginger, H. Chen, A. K. Y. Jen, *Nat. Nanotechnol.* **2022**, *17*, 53.

[86] X. Duan, W. Song, J. Qiao, X. Li, Y. Cai, H. Wu, J. Zhang, X. Hao, Z. Tang, Z. Ge, F. Huang, Y. Sun, *Energy Environ. Sci.* **2022**, *15*, 1563.

[87] S. Guan, Y. Li, K. Yan, W. Fu, L. Zuo, H. Chen, *Adv. Mater.* **2022**, *34*, 2205844.

[88] C. He, Z. Bi, Z. Chen, J. Guo, X. Xia, X. Lu, J. Min, H. Zhu, W. Ma, L. Zuo, H. Chen, *Adv. Funct. Mater.* **2022**, *32*, 2112511.

[89] W. Feng, S. Wu, H. Chen, L. Meng, F. Huang, H. Liang, J. Zhang, Z. Wei, X. Wan, C. Li, Z. Yao, Y. Chen, *Adv. Energy Mater.* **2022**, *12*, 2104060.

[90] B. Fan, W. Gao, X. Wu, X. Xia, Y. Wu, F. R. Lin, Q. Fan, X. Lu, W. J. Li, W. Ma, A. K. Y. Jen, *Nat. Commun.* **2022**, *13*, 5946.

[91] R. Yu, X. Wei, G. Wu, T. Zhang, Y. Gong, B. Zhao, J. Hou, C. Yang, Z. Tan, *Energy Environ. Sci.* **2022**, *15*, 822.

[92] Y. Cui, Y. Xu, H. Yao, P. Bi, L. Hong, J. Zhang, Y. Zu, T. Zhang, J. Qin, J. Ren, Z. Chen, C. He, X. Hao, Z. Wei, J. Hou, *Adv. Mater.* **2021**, *33*, 2102420.

[93] J. Zhang, F. Bai, I. Angunawela, X. Xu, S. Luo, C. Li, G. Chai, H. Yu, Y. Chen, H. Hu, Z. Ma, H. Ade, H. Yan, *Adv. Energy Mater.* **2021**, *11*, 2102596.

[94] J. Song, L. Zhu, C. Li, J. Xu, H. Wu, X. Zhang, Y. Zhang, Z. Tang, F. Liu, Y. Sun, *Matter* **2021**, *4*, 2542.

[95] Y. Li, J. Song, Y. Dong, H. Jin, J. Xin, S. Wang, Y. Cai, L. Jiang, W. Ma, Z. Tang, Y. Sun, *Adv. Mater.* **2022**, *34*, 2110155.

[96] S. Mathew, A. Yella, P. Gao, R. Humphry-Baker, B. F. E. Curchod, N. Ashari-Astani, I. Tavernelli, U. Rothlisberger, M. K. Nazeeruddin, M. Grätzel, *Nat. Chem.* **2014**, *6*, 242.

[97] P.-H. Chang, M. C. Sil, K. S. K. Reddy, C.-H. Lin, C.-M. Chen, *ACS Appl. Mater. Interfaces* **2022**, *14*, 25466.

[98] A. K. Bharwal, L. Manceriu, C. Olivier, A. Mahmoud, C. Iojoiu, T. Toupance, C. M. Ruiz, M. Pasquinelli, D. Duché, J.-J. Simon, C. Henrist, F. Alloin, *Chem. Eng. J.* **2022**, *446*, 136777.

[99] C. Liao, H. Wu, H. Tang, L. Wang, D. Cao, *Sol. Energy* **2022**, *240*, 399.

[100] R. Tang, S. Chen, Z.-H. Zheng, Z.-H. Su, J.-T. Luo, P. Fan, X.-H. Zhang, J. Tang, G.-X. Liang, *Adv. Mater.* **2022**, *34*, 2109078.

[101] Y. Wang, L. Peng, Z. Wang, G. Konstantatos, *Adv. Energy Mater.* **2022**, *12*, 2200700.

[102] C. Jiang, J. Zhou, R. Tang, W. Lian, X. Wang, X. Lei, H. Zeng, C. Zhu, W. Tang, T. Chen, *Energy Environ. Sci.* **2021**, *14*, 359.

[103] S. Wang, Y. Zhao, B. Che, C. Li, X. Chen, R. Tang, J. Gong, X. Wang, G. Chen, T. Chen, J. Li, X. Xiao, *Adv. Mater.* **2022**, *34*, 2206242.

[104] Y. Wu, P. Zheng, J. Peng, M. Xu, Y. Chen, S. Surve, T. Lu, A. D. Bui, N. Li, W. Liang, L. Duan, B. Li, H. Shen, T. Duong, J. Yang, X. Zhang, Y. Liu, H. Jin, Q. Chen, T. White, K. Catchpole, H. Zhou, K. Weber, *Adv. Energy Mater.* **2022**, *12*, 2200821.

[105] K. Liu, B. Chen, Z. J. Yu, Y. Wu, Z. Huang, X. Jia, C. Li, D. Spronk, Z. Wang, Z. Wang, S. Qu, Z. C. Holman, J. Huang, *J. Mater. Chem. A* **2022**, *10*, 1343.

[106] M. Jošt, E. Köhnen, A. Al-Ashouri, T. Bertram, Š. Tomšič, A. Magomedov, E. Kasparavicius, T. Kodalle, B. Lipovšek, V. Getautis, R. Schlatmann, C. A. Kaufmann, S. Albrecht, M. Topič, *ACS Energy Lett.* **2022**, *7*, 1298.

[107] K. Datta, J. Wang, D. Zhang, V. Zardetto, W. H. M. Remmerswaal, C. H. L. Weijtens, M. M. Wienk, R. A. J. Janssen, *Adv. Mater.* **2022**, *34*, 2110053.

[108] H. Gao, Q. Lu, K. Xiao, Q. Han, R. Lin, Z. Liu, H. Li, L. Li, X. Luo, Y. Gao, Y. Wang, J. Wen, Z. Zou, Y. Zhou, H. Tan, *Sol. RRL* **2021**, *5*, 2100814.

[109] J. Wang, V. Zardetto, K. Datta, D. Zhang, M. M. Wienk, R. A. J. Janssen, *Nat. Commun.* **2020**, *11*, 5254.

[110] Y. Huang, L. Meng, H. Liang, M. Li, H. Chen, C. Jiang, K. Zhang, F. Huang, Z. Yao, C. Li, X. Wan, Y. Chen, *J. Mater. Chem. A* **2022**, *10*, 11238.

[111] Z. Zheng, J. Wang, P. Bi, J. Ren, Y. Wang, Y. Yang, X. Liu, S. Zhang, J. Hou, *Joule* **2022**, *6*, 171.

[112] S. H. Kang, M. J. Jeong, Y. K. Eom, I. T. Choi, S. M. Kwon, Y. Yoo, J. Kim, J. Kwon, J. H. Park, H. K. Kim, *Adv. Energy Mater.* **2017**, *7*, 1602117.

[113] M. A. Green, K. Emery, Y. Hishikawa, W. Warta, E. D. Dunlop, *Prog. Photovoltaics* **2013**, *21*, 1.

[114] M. A. Green, E. D. Dunlop, J. Hohl-Ebinger, M. Yoshita, N. Kopidakis, X. Hao, *Prog. Photovoltaics* **2021**, *29*, 657.

[115] M. A. Green, K. Emery, Y. Hishikawa, W. Warta, E. D. Dunlop, D. H. Levi, A. W. Y. Ho-Baillie, *Prog. Photovoltaics* **2017**, *25*, 3.

[116] Y. Wang, T. Li, X. Chen, L. Zhang, *Mater. Lett.* **2022**, *321*, 132460.

[117] M. Chen, Q. Dong, C. Xiao, X. Zheng, Z. Dai, Y. Shi, J. M. Luther, N. P. Padture, *ACS Energy Lett.* **2022**, *7*, 2256.

[118] Z. Zheng, F. Li, J. Gong, Y. Ma, J. Gu, X. Liu, S. Chen, M. Liu, *Adv. Mater.* **2022**, *34*, 2109879.

[119] L. Yang, J. Feng, Z. Liu, Y. Duan, S. Zhan, S. Yang, K. He, Y. Li, Y. Zhou, N. Yuan, J. Ding, S. Liu, *Adv. Mater.* **2022**, *34*, 2201681.

[120] S. Wu, Z. Li, J. Zhang, X. Wu, X. Deng, Y. Liu, J. Zhou, C. Zhi, X. Yu, W. C. H. Choy, Z. Zhu, A. K. Y. Jen, *Adv. Mater.* **2021**, *33*, 2105539.

[121] X. Meng, X. Hu, Y. Zhang, Z. Huang, Z. Xing, C. Gong, L. Rao, H. Wang, F. Wang, T. Hu, L. Tan, Y. Song, Y. Chen, *Adv. Funct. Mater.* **2021**, *31*, 2106460.

[122] B. Fan, J. Xiong, Y. Zhang, C. Gong, F. Li, X. Meng, X. Hu, Z. Yuan, F. Wang, Y. Chen, *Adv. Mater.* **2022**, *34*, 2201840.

[123] Q. Dong, M. Chen, Y. Liu, F. T. Eickemeyer, W. Zhao, Z. Dai, Y. Yin, C. Jiang, J. Feng, S. Jin, S. Liu, S. M. Zakeeruddin, M. Grätzel, N. P. Padture, Y. Shi, *Joule* **2021**, *5*, 1587.

[124] P. Sun, J. Qu, Q. Hu, Y. Ma, H. Liu, Z.-X. Xu, Z. Huang, *ACS Appl. Energy Mater.* **2022**, *5*, 3568.

[125] Y. Han, Z. Hu, W. Zha, X. Chen, L. Yin, J. Guo, Z. Li, Q. Luo, W. Su, C.-Q. Ma, *Adv. Mater.* **2022**, *34*, 2110276.

[126] Z. Chen, W. Song, K. Yu, J. Ge, J. Zhang, L. Xie, R. Peng, Z. Ge, *Joule* **2021**, *5*, 2395.

[127] Y. Chen, J. Wan, G. Xu, X. Wu, X. Li, Y. Shen, F. Yang, X. Ou, Y. Li, Y. Li, *Sci China Chem* **2022**, *65*, 1164.

[128] N. Cui, Y. Song, C.-H. Tan, K. Zhang, X. Yang, S. Dong, B. Xie, F. Huang, *npj Flexible Electron.* **2021**, *5*, 31.

[129] B. Murali, K. Gireesh Baiju, R. Krishna Prasad, K. Jayanarayanan, D. Kumaresan, *Sustainable Energy Fuels* **2022**, *6*, 2503.

[130] H. Lai, J. Luo, Y. Zwirner, S. Olthof, A. Wieczorek, F. Ye, Q. Jeangros, X. Yin, F. Akhundova, T. Ma, R. He, R. K. Kothandaraman, X. Chin, E. Gilshtein, A. Müller, C. Wang, J. Thiesbrummel, S. Siol, J. M. Prieto, T. Unold, M. Stolterfoht, C. Chen, A. N. Tiwari, D. Zhao, F. Fu, *Adv. Energy Mater.* **2022**, *12*, 2202438.

[131] L. Sun, W. Wang, L. Hao, Z. Jia, Y. Zhao, G. Zhi, H. Yao, *Mater. Sci. Semicond. Process.* **2022**, *138*, 106301.

[132] L. Sun, W. Wang, L. Hao, A. Raza, Y. Zhao, Z. Tang, G. Zhi, H. Yao, *Ceram. Int.* **2022**, *48*, 19891.

[133] W. Xie, Q. Sun, Q. Yan, J. Wu, C. Zhang, Q. Zheng, Y. Lai, H. Deng, S. Cheng, *Small* **2022**, *18*, 2201347.

[134] Q. Zhao, H. Shen, Y. Xu, K. Gao, D. Chen, Y. Li, *ACS Appl. Energy Mater.* **2022**, *5*, 3668.

[135] D.-Y. Jung, Y.-R. Jeong, M. S. Mina, S.-E. Lee, E. Enkhbayar, J. Kim, *Curr. Appl. Phys.* **2022**, *41*, 66.

[136] S. Pouladi, C. Favela, W. Wang, M. Moradnia, N.-I. Kim, S. Shervin, J. Chen, S. Sharma, G. Yang, M.-C. Nguyen, R. Choi, J. Kim, A. Fedorenko, B. Bogner, J. Bao, S. M. Hubbard, V. Selvamanickam, J.-H. Ryou, *Sol. Energy Mater. Sol. Cells* **2022**, *243*, 111791.

[137] W. L. Rance, J. M. Burst, D. M. Meysing, C. A. Wolden, M. O. Reese, T. A. Gessert, W. K. Metzger, S. Garner, P. Cimo, T. M. Barnes, *Appl. Phys. Lett.* **2014**, *104*, 143903.

[138] B. Tyagi, H. B. Lee, N. Kumar, W.-Y. Jin, K.-J. Ko, M. M. Ovhal, R. Sahani, H.-J. Chung, J. Seo, J.-W. Kang, *Nano Energy* **2022**, *95*, 106978.

[139] S. Seo, K. Akino, J.-S. Nam, A. Shawky, H.-S. Lin, H. Nagaya, E. I. Kauppinen, R. Xiang, Y. Matsuo, I. Jeon, S. Maruyama, *Adv. Mater. Interfaces* **2022**, *9*, 2101595.

[140] S. Yoon, H. U. Ha, H.-J. Seok, H.-K. Kim, D.-W. Kang, *Adv. Funct. Mater.* **2022**, *32*, 2111760.

[141] S. Lie, A. Bruno, L. H. Wong, L. Etgar, *ACS Appl. Mater. Interfaces* **2022**, *14*, 11339.

[142] D. Han, S. Han, Z. Bu, Y. Deng, C. Liu, W. Guo, *Sol. RRL* **2022**, *6*, 2200441.

[143] L. Zheng, M. Li, S. Dai, Y. Wu, Y. Cai, X. Zhu, S. Ma, D. Yun, J.-F. Li, *J. Phys. Chem. C* **2021**, *125*, 18623.

[144] W. Liu, S. Sun, L. Zhou, Y. Cui, W. Zhang, J. Hou, F. Liu, S. Xu, X. Zhu, *Angew. Chem., Int. Ed.* **2022**, *61*, 202116111.

[145] S. Liu, H. Li, X. Wu, D. Chen, L. Zhang, X. Meng, L. Tan, X. Hu, Y. Chen, *Adv. Mater.* **2022**, *34*, 2201604.

[146] X. Yuan, R. Sun, Y. Wu, T. Wang, Y. Wang, W. Wang, Y. Yu, J. Guo, Q. Wu, J. Min, *Adv. Funct. Mater.* **2022**, *32*, 2200107.

[147] H. I. Jeong, S. Biswas, S. C. Yoon, S.-J. Ko, H. Kim, H. Choi, *Adv. Energy Mater.* **2021**, *11*, 2102397.

[148] J. Jing, S. Dong, K. Zhang, Z. Zhou, Q. Xue, Y. Song, Z. Du, M. Ren, F. Huang, *Adv. Energy Mater.* **2022**, *12*, 2200453.

**ADVANCED
SCIENCE NEWS**

www.advancedsciencenews.com

**ADVANCED
ENERGY
MATERIALS**

www.advenergymat.de

[149] X. Huang, L. Zhang, Y. Cheng, J. Oh, C. Li, B. Huang, L. Zhao, J. Deng, Y. Zhang, Z. Liu, F. Wu, X. Hu, C. Yang, L. Chen, Y. Chen, *Adv. Funct. Mater.* **2022**, *32*, 2108634.

[150] D. Wang, Y. Li, G. Zhou, E. Gu, R. Xia, B. Yan, J. Yao, H. Zhu, X. Lu, H.-L. Yip, H. Chen, C.-Z. Li, *Energy Environ. Sci.* **2022**, *15*, 2629.

[151] X. Xie, Y. Zhang, Y. Ren, L. He, Y. Yuan, J. Zhang, P. Wang, *J. Phys. Chem. C* **2022**, *126*, 11007.

[152] F. Odobel, T. Baron, W. Naim, I. Nikolinakos, B. Andrin, Y. Pellegrin, D. Jacquemin, S. Haacke, F. Sauvage, *Angew. Chem., Int. Ed.* **2022**, *61*, 202207459.

[153] C. Yang, M. Moemeni, M. Bates, W. Sheng, B. Borhan, R. R. Lunt, *Adv. Opt. Mater.* **2020**, *8*, 1901536.

[154] Y. Zhao, R. R. Lunt, *Adv. Energy Mater.* **2013**, *3*, 1143.

[155] Y. Zhao, G. A. Meek, B. G. Levine, R. R. Lunt, *Adv. Opt. Mater.* **2014**, *2*, 606.

[156] J. Sanchez-Diaz, R. S. Sánchez, S. Masi, M. Krečmarová, A. O. Alvarez, E. M. Barea, J. Rodriguez-Romero, V. S. Chirvony, J. F. Sánchez-Royo, J. P. Martinez-Pastor, I. Mora-Seró, https://emerging-pv.org/wp-content/uploads/2022/06/Add_SI_Stability-PSC_Joule.2022.02.014.pdf (accessed: June 2022).

[157] Q. Zhou, C. Cai, Q. Xiong, Z. Zhang, J. Xu, L. Liang, S. Wang, W. Sun, Z. Yuan, P. Gao, *Adv. Energy Mater.* **2022**, *12*, 2201243.